This is a non-peer reviewed pre-print of *The role of the Hikurangi subduction interface in enabling Kaikōura-like earthquakes: Insights from synthetic earthquake catalogues,* by Camilla Penney, Andrew Howell, Timothy McLennan, Andrew Nicol and Bill Fry, submitted to Seismica.

The role of the Hikurangi subduction interface in enabling Kaikōura-like earthquakes: Insights from synthetic earthquake catalogues

Camilla Penney * [1], **Andrew Howell** [1,2], **Timothy McLennan** [3], **Andrew Nicol** [1], **Bill Fry** [2]

[1]Te Kura Aronukurangi | School of Earth and Environment, Te Whare Wānanga O Waitaha | University of Canterbury, Christchurch, Aotearoa New Zealand, [2]Earth Sciences New Zealand, Lower Hutt, Aotearoa New Zealand, [3]Seequent, The Bentley Subsurface Company

Author contributions: *Conceptualization*: CP, AH, AN. *Software*: CP, AH, TM. *Investigation*: CP, AH. *Writing - Original draft*: CP. *Writing - Review & Editing*: CP, AN, AH. *Funding acquisition*: AN,BF.

Abstract A well-known problem in seismic hazard is the short duration of the historical record relative to the time between large earthquakes. This short record means that not all possible earthquakes have been observed, and that the statistics of earthquake recurrence intervals and magnitudes are poorly constrained. These issues are particularly acute for earthquakes involving multiple faults, such as the 2010 El Mayor-Cucapah and 2016 Kaikōura earthquakes. Such earthquakes demonstrate the potentially complex interactions of faults in single earthquakes, contrasting with the typical assumption of characteristic fault ruptures used in seismic hazard assessment. Physics-based earthquake simulators offer one approach for exploring the occurrence of, and controls on, such multi-fault earthquakes. Here we use the physics-based earthquake simulator RSQsim to generate two 450 kyr synthetic earthquake catalogues for central Aotearoa New Zealand, with and without the Hikurangi subduction interface. We improve on previous synthetic earthquake catalogues for Aotearoa New Zealand by implementing a new 3D fault modelling methodology, which is better able to account for along-fault and down-dip variations in fault geometry. We investigate the occurrence of multi-fault earthquakes in our synthetic catalogues with a particular emphasis on the role of the southern part of the Hikurangi subduction interface in these earthquakes. The synthetic catalogues show an increasing proportion of multi-fault earthquakes at higher magnitudes. We find that the subduction interface exerts a significant control on the aspect ratios, rates of occurrence, and faults involved in synthetic multi-fault earthquakes. Whilst our catalogues contain >100 complex multi-fault events broadly similar to the 2016 Kaikōura earthquake, none rupture exactly the same combination of faults, suggesting that either this fault combination is rare or that key aspects of the controlling physics or fault network are not captured by the earthquake simulator.

Non-technical summary Earthquakes are caused by the movement of tectonic plates. These tectonic plates only move as fast as fingernails grow, but in an earthquake the ground might move by up to tens of metres. The difference between the slow movement of plates and fast movement in earthquakes means that earthquakes do not move the same fault very often, so human observations are typically only a few earthquakes long. To understand what kinds of earthquakes could happen, even if we haven't seen them yet, we used a computer model of the how plate movement leads to earthquakes on the faults in central Aotearoa-New Zealand. We investigated how much difference having a subduction zone offshore of the northern South Island would have on these size, number and shape of these earthquakes and how many different faults are involved in them. In our models the subduction zone makes a big difference to which faults move together in the same earthquake and the similarity of these synthetic earthquakes to the 2016 Kaikōura earthquake. Learning more about where the subduction zone is and whether it can move in earthquakes, either on its own or with faults in the plate above it, is very important for understanding earthquake risk in Aotearoa-New Zealand.

1 Introduction

The historical record of large earthquakes is often much shorter than inferred geological recurrence intervals. Although there is potential to enhance this record (e.g. Nunn, 2003; Downes, 2004; Rollins et al., 2025), it remains the case that in many places, such as Aotearoa New Zealand (A-NZ), human observations, particularly those constrained by instrumental data, are unlikely to provide a complete overview of the types of earthquakes which can occur, or the earthquake-capable faults in a particular region (Nicol et al., 2016). Whilst paleoseismic data can extend the seismic record to thousands of years, no such records currently span more than 24 earthquakes (Hokuri Creek, Alpine Fault, A-NZ; Berryman et al., 2012) meaning that the distribution of interevent times remains poorly constrained. Further, recurrence intervals and magnitudes derived from pale-

*Corresponding author: camilla.penney@canterbury.ac.nz

oseismic data depend on assumptions about the scaling of earthquake-surface ruptures, which allow observations at a single point to be interpreted in terms of entire earthquakes. Such interpretations are typically made assuming that each earthquake ruptures a single fault, following scaling relations between mean fault slip, magnitude and area (e.g. Wells and Coppersmith, 1994; Stirling et al., 2013; Anderson et al., 2021; Stirling et al., 2023).

Recent observations of earthquakes rupturing multiple distinct faults, such as the 2010 El-Mayor Cucapah (e.g. Fletcher et al., 2014) and 2016 Kaikōura earthquakes (Hamling et al., 2017, section 2;), as well as complex traces of historical events (e.g. Abdrakhmatov et al., 2016), have called into question the assumption of characteristic earthquakes on faults with particular dimensions. To date, such earthquakes rupturing multiple distinct faults ('multi-fault' earthquakes) have predominantly been defined by their surface ruptures (e.g. Litchfield et al., 2018), but this may lead to underestimates of the number of events actually involving multiple faults, since slip may not reach the surface on all faults involved in a given earthquake (e.g. Beavan et al., 2010, 2012). From a seismic hazard perspective it is important to understand how frequently multi-fault earthquakes occur, which faults are capable of co-rupture and what controls this synchronous seismicity (Page, 2021; Howell et al., 2023a).

Physics-based earthquake simulators offer a potential approach to addressing these questions (Tullis et al., 2012b; Field, 2019). By using approximations to current understandings of the frictional controls on earthquake rupture, simulators are able to generate catalogues of synthetic earthquakes on timescales much longer than the observational record. Simulators also offer the potential to test the sensitivity of synthetic earthquake catalogues to particular parameters, such as friction coefficients (Liao et al., 2024), fault roughness (Delogkos et al., 2023) and fault-network geometry. In particular, recent advances in the generation of 3D fault models (Howell et al., in review) open the possibility of using such simulators with multiple geometric configurations.

Since the occurrence rate of complex multi-fault earthquakes is likely to be a function of a specific fault system, we focus on an area where such earthquakes are known to occur, and where earthquake simulators have the potential to contribute to outstanding debates about the frequency of such events, namely central A-NZ. This region, which spans the northern South Island | Te Waipounamu and southern North Island | Te Ika-a-Māui (Figure 1), includes the epicentral region of the 2016 Kaikōura earthquake, as well as the 2010 Darfield and 2011 Christchurch earthquakes. In addition to being an area at the centre of discussions on multi-fault earthquakes (e.g. Hamling et al., 2017; Quigley et al., 2019; Ando and Kaneko, 2018), this region has the advantage of having numerous well-mapped faults, with well-defined slip rates (Seebeck et al., 2023), many of which have been extensively studied paleoseismologically (e.g. Van Dissen and Yeats, 1991; Van Dissen and Nicol, 2009; Little et al., 2018; Hatem et al., 2019; Morris et al., 2023a,b; Langridge et al., 2023; Humphrey et al., 2025).

We use a multi-fault, multi-cycle earthquake simulator (RSQsim; Richards-Dinger and Dieterich, 2012) to investigate three key questions about the occurrence of multi-fault earthquakes in central A-NZ: 1) how common are multi-fault ruptures? 2) Can RSQsim produce synthetic earthquakes with similar properties to the 2016 Kaikōura earthquake? and 3) what is the role of the Hikurangi subduction interface in controlling the proportion of earthquakes which are multi-fault and the recurrence interval, magnitude and geometry of such earthquakes?

To address these questions, we first summarise the key features of the 2016 Kaikōura earthquake in the context of the regional tectonics of central A-NZ (Section 2). We then present methods for developing an improved 3D model of the fault network in central A-NZ and an associated catalogue of synthetic earthquakes (Section 3). In Section 4 we outline the main ensemble properties of this synthetic earthquake catalogue and a version without the subduction interface. We then investigate the properties of multi-fault earthquakes in these synthetic catalogues, with specific focus on synthetic earthquakes analogous to that which occurred in Kaikōura in 2016. Finally, we discuss the implications of these results for our understanding of (complex) multi-fault earthquakes (Section 5).

2 Regional tectonics and the 2016 Kaikōura earthquake

The 2016 Kaikōura earthquake, which provides the motivation for this study, occurred in central A-NZ (Figure 1). This area spans the north-south transition along the Pacific - Australia plate boundary from subduction, along the Hikurangi margin, to oblique right-lateral continental collision, on the Alpine Fault (e.g. Wallace et al., 2012). This transition is accommodated by a region of complex continental faulting on dominantly right-lateral faults in the Marlborough fault system and the gradual transfer of slip on the subduction megathrust to these onshore faults (Anderson et al., 1993; Walcott, 1998; Little and Jones, 1998; Wallace et al., 2012; Upton et al., 2025).

The Kaikōura earthquake initiated on The Humps fault in North Canterbury (Nicol et al., 2018) and ruptured into the south-eastern end of the Marlborough fault system as far north as the Kekerengu and Needles faults (Figure 1), crossing the boundary between what had previously been considered to be two distinct tectonic domains (Stirling et al., 2012; Hamling et al., 2017; Stirling et al., 2017). In doing so, however, no significant rupture (i.e. <0.2 m of slip) was observed on the Hope fault (e.g. Hamling et al., 2017), which had been thought to act as the domain boundary (Stirling et al., 2012). The lack of rupture of the Hope fault during the Kaikōura earthquake has proved particularly challenging for dynamic models of the earthquake to reproduce, leading to competing hypotheses about the likely stress state of the Hope fault prior to the event (Ando and

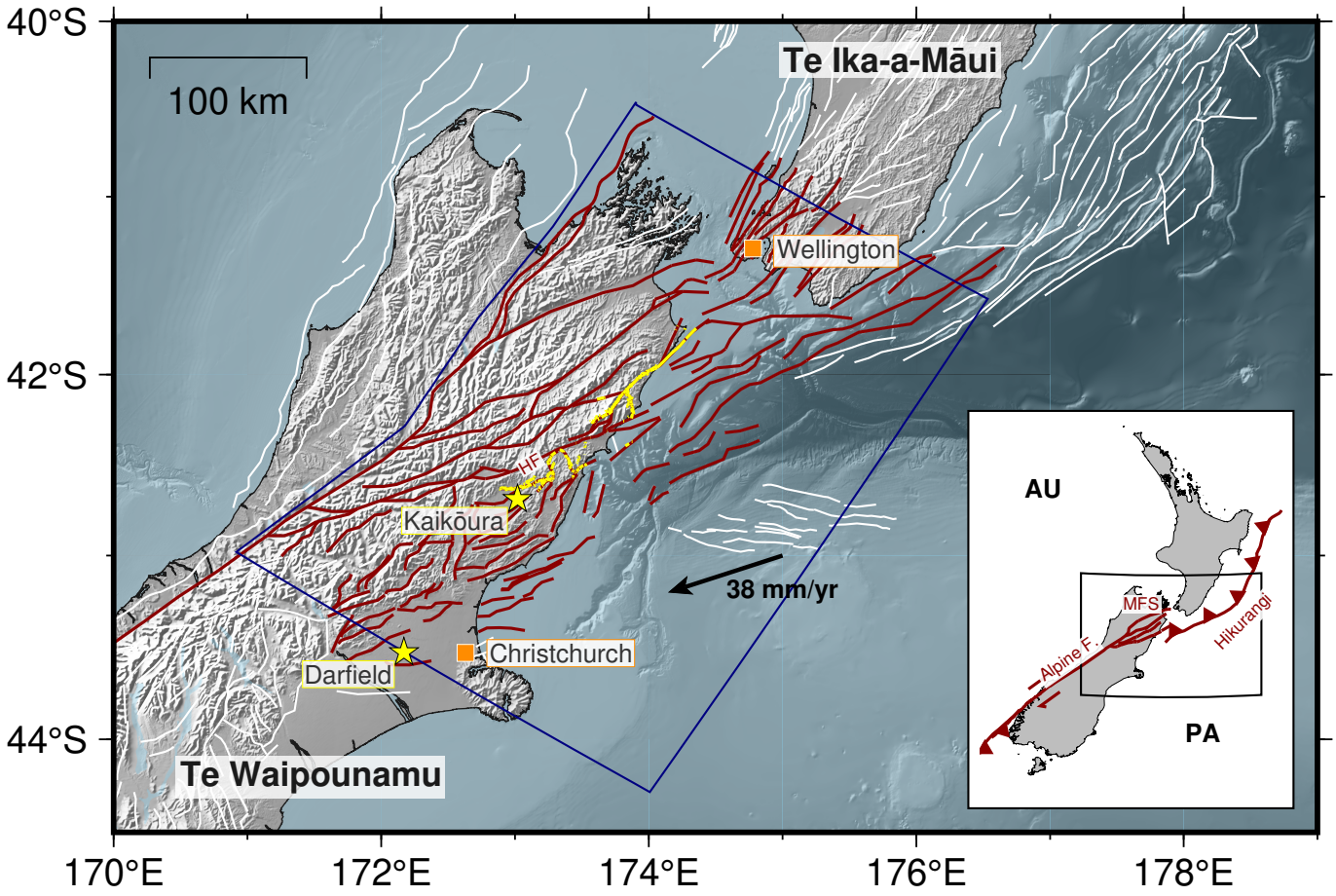

Figure 1 Map of the study area, which spans the northern South Island | Te Waipounamu and southern North Island | Te Ika-a-Māui of A-NZ. Fault traces from the New Zealand Community Fault Model (Seebeck et al., 2022, 2023) are shown in white, whilst those used in our modelling are shown in red. The faults used are those within, or which intersect, the blue box. We exclude faults with reported slip rates of 0 mm yr^{-1}, except those which are thought to have ruptured in the Kaikōura earthquake (e.g. the Offshore Splay Thrust Fault, Mouslopoulou et al., 2019; Nicol et al., 2023). Surfaces ruptures from this earthquake (downloaded from https://data.gns.cri.nz/af/, last accessed 4/12/25) are shown in yellow, which extend from The Humps fault (the epicentre of the earthquake, shown by the yellow star labelled Kaikōura) to the Needles fault in the north east. The plate motion vector is taken from DeMets et al. (2010). HF is the Hope Fault. Yellow star on the edge of the blue box shows the epicentre of the 2010 Darfield earthquake. Inset shows the overall tectonics of A-NZ, on the boundary between the Pacific (PA) and Australian (AU) plates, transitioning from the Hikurangi subduction zone in the north-east, through the Marlborough fault zone (MFS) to the Alpine Fault and the Puysegur subduction zone in the south-west. Black box shows the location of the main figure.

Kaneko, 2018; Ulrich et al., 2019). Whether or not such ruptures are likely to be observed in our synthetic earthquake catalogues depends on whether the dynamic or static stress state is the primary control on the involvement of fast-slipping faults in multi-fault earthquakes (discussed further in section 3).

How often the faults which ruptured (and did not rupture) in the Kaikōura earthquake move in complex multi-fault, as opposed to single fault or simpler multi-fault, earthquakes is unclear. Litchfield et al. (2018) and Nicol et al. (2018) proposed a minimum return period of 6,000 years based on an estimated vertical slip rate for The Humps fault of 0.2 ± 0.1 mm yr^{-1} (the slowest slipping fault involved in the earthquake, on which the rupture nucleated Barrell and Townsend, 2012). Brough et al. (2023) conducted detailed paleoseismic investigations of The Humps fault and revised its recurrence interval to 1.8–3.4 kyr, potentially decreasing the minimum return period of Kaikōura-like events to ~2 kyr. However, it is also possible that not all earthquakes on The Humps fault are complex, multi-fault ruptures. Walsh et al. (2023) used a set of probabilities for fault co-rupture combined with Monte Carlo simulations to estimate the proportion of ruptures initiating on The Humps fault which propagate to the Kekerengu fault. Their preferred model suggests that only 1 out of 250,000 earthquakes initiating on The Humps propagate as far as the Kekerengu fault, which would suggest much longer recurrence intervals for Kaikōura-like earthquakes. Although Walsh et al. (2023)'s results are dependent on the precise rules used to determine fault co-rupture probabilities, and likely represent a lower bound since their model does not incorporate three-dimensional fault connectivity, they suggest that the recurrence interval for the specific faults involved in the 2016 Kaikōura earthquake to rupture in a single earthquake could be up to 100s kyrs.

What proportion of earthquakes on a given fault in

Marlborough / North Canterbury are complex, multi-fault events is a key question for seismic hazard across the region (e.g. Howell et al., 2023a). Inconsistencies between the mapped rake of the Jordan thrust (Van Dissen and Yeats, 1991) and its sense of motion in the Kaikōura earthquake, as well as the observed 8 m of surface displacement on the previously unmapped Papatea fault (Langridge et al., 2018), suggest that the motion of these faults in the Kaikōura earthquake might not reflect their long-term or 'usual' slip behaviour (Howell et al., 2020). The relatively subdued topography associated with the Papatea fault has also led to suggestions that the fault may not be well described by elastic models of fault recurrence (Hamling et al., 2017; Diederichs et al., 2019), and that the fault may rupture predominantly in complex, multi-fault earthquakes (Langridge et al., 2018, 2023). This lack of geomorphic expression also provides a potential lower bound on the recurrence interval of Kaikōura-like earthquakes, since any associated topography must be significantly eroded between events (Langridge et al., 2018). The first key question which we investigate with our simulations is, therefore, how common are multi-fault ruptures?

The 2016 earthquake has been almost ubiquitously described as "complex" (e.g. Hollingsworth et al., 2017; Hamling et al., 2017; Cesca et al., 2017; Stirling et al., 2017; Xu et al., 2018; Ando and Kaneko, 2018; Nicol et al., 2022), referring primarily to the large number of faults involved, and to differences in their orientation and sense of motion (e.g. Nicol et al., 2018; Kearse et al., 2018). Offsets $>$0.5 m were observed on 20 separate surface-rupturing faults (Litchfield et al., 2018), with $\geq$14 faults having surface rupture over at least 1 km of their traces (Stirling et al., 2017; Litchfield et al., 2018). The second question we investigate is therefore whether a quasi-static earthquake simulator can produce synthetic earthquakes with characteristics similar to those of the 2016 Kaikōura earthquake.

In addition to the surface ruptures, slip at depth and blind faults may also have played an important role in linking the faults involved. Nicol et al. (2023) concluded that the faults involved in the Kaikōura earthquake are effectively hard-linked at depth, which Schwartz (2018) and Nicol et al. (2022) argued is likely to be a more general property of multi-fault earthquakes. Earthquake simulators provide an opportunity to test the importance of this connectivity in controlling the occurrence of complex multi-fault earthquakes.

A critical fault with the potential to provide hard-linking at depth is the Hikurangi subduction interface (Figure 1). The role of the Hikurangi subduction interface in the Kaikōura earthquake has been widely debated (e.g. Hamling et al., 2017; Bai et al., 2017; Clark et al., 2017; Lamb et al., 2018; Wang et al., 2018; Mouslopoulou et al., 2019; Herman et al., 2023). The interface is at depths of 25-30 km beneath The Humps fault (Williams et al., 2013), but how, and even whether, it connects to the crustal faults which dominated the moment release in the earthquake is not well resolved (Nicol et al., 2023). There is general agreement in the literature, based on: vertical coastal motions (Clark et al., 2017; Howell and Clark, 2022; Nicol et al., 2023), teleseismic waveforms (Hollingsworth et al., 2017; Duputel and Rivera, 2017; Bai et al., 2017), geodesy (Hamling et al., 2017; Lamb et al., 2018), tsunami observations (Bai et al., 2017) and earthquake relocations (Cesca et al., 2017; Chamberlain et al., 2021), that coseismic slip is likely to have occurred on one or more offshore blind thrust faults. However, whether this slip occurred on the interface itself (Bai et al., 2017; Herman et al., 2023), on one of several proposed steeper dipping splay faults (e.g. the Point Kean fault, Clark et al. (2017); the Offshore Splay Thrust fault, Mouslopoulou et al., 2019; Nicol et al., 2022), or a combination of these, remains unresolved (and may ultimately be unresolvable within the uncertainties of the geometry of the interface and observational constraints; Wallace et al., 2017). Geodetic measurements following the 2016 Kaikōura earthquake conclusively demonstrate widespread afterslip on the southernmost part of the mapped subduction interface (Wallace et al., 2018; Mouslopoulou et al., 2019; Zhang et al., 2025). However, several studies have also argued that features initially proposed to require slip on the subduction interface, such as the non-double couple component of the moment tensor, could be explained equally well by slip on a splay fault (Cesca et al., 2017). Uncertainty surrounding the role of the subduction interface in the Kaikōura earthquake (Section 2) has led to significant interest in the potential for combined subduction interface - upper crustal multi-fault earthquakes, and their contribution to seismic hazard (e.g. Clark et al., 2019; Pizer et al., 2023; Coffey et al., 2023; Humphrey et al., 2025).

Resolving the role of the Hikurangi subduction interface in the 2016 Kaikōura earthquake is also important for understanding how the subduction zone terminates at its southern end. The southwards increase in the obliquity of the Pacific-Australia collision and progressively higher proportion of plate motion accommodated by the Marlborough fault system had led to the suggestion that the subduction zone might be "permanently locked", that is, not seismogenic, on timescales of 10s - 100s kyrs (Reyners, 1998). However, the Benioff zone, and tomographic signature of the subducting Pacific Plate extend at least as far south as Christchurch (Eberhart-Phillips and Reyners, 1997; Eberhart-Phillips et al., 2010; Reyners et al., 2011). Several geodetic studies (Wallace et al., 2009, 2012) and uplifted marine terraces (Ota et al., 1996) also suggest the possibility of offshore deformation. Hamling et al. (2022) argued that coastal subsidence of eastern Marlborough based on InSAR timeseries is consistent with interplate coupling and seismic slip on the subduction interface. Combined with the observation of afterslip and possible coseismic movement of the subduction interface in 2016, these lines of evidence suggest that the interface may be able to slip further south than had previously been anticipated. The lack of megathrust earthquakes observed to date might be related to observation times and slow rates of convergence and/or to the limited resolution of available data (e.g., both the 1855 M_w8.2 Wairarapa earthquake and the 2016 M_w7.8 Kaikōura earthquake may have ruptured the subduction interface), rather than a lack of seismogenic potential, which would have

important implications for seismic and tsunami hazard in the South Island | Te Waipounamu (Van Dissen et al., 2022, 2024; Gerstenberger et al., 2024a).

Equally, if a hard-linking structure, such as the subduction interface, is required to allow multi-fault rupture, or has a significant impact on which faults are able to rupture together, it would have important implications for how the viability of particular multi-fault earthquakes is assessed in seismic hazard modelling (e.g. Milner et al., 2022). Many recent seismic hazard models (such as UCERF3 and the 2022 New Zealand National Seismic Hazard model Field et al., 2017; Gerstenberger et al., 2022, 2024a) use plausibility filters based on surface traces and Coulomb stress modelling to assess this rupture viability, which may not provide a good representation of the full range of possible ruptures (e.g. Page, 2021), particularly if there are unmapped linking faults or poorly-resolved 3D fault geometries.

Debate about the involvement of the subduction interface, and the importance of understanding fault connectivity for seismic hazard, leads to the final question we investigate with our simulations: what is the role of the Hikurangi subduction interface in controlling the proportion of earthquakes which are multi-fault and the recurrence interval, magnitude and geometry of such earthquakes?

3 Generating Synthetic Earthquake Catalogues

To investigate the occurrence, and frequency of Kaikōura-like earthquakes we generate two synthetic earthquake catalogues using a multi-fault, multicycle earthquake simulator, RSQsim (Richards-Dinger and Dieterich, 2012). Below we briefly introduce the simulator, before outlining the steps involved in our model construction.

3.1 RSQsim

Tullis et al. (2012b) describe earthquake simulators as "computer programs that use [the] physics of stress transfer and frictional resistance to describe earthquake sequences", with different simulators using different simplifications to this physics in order to make the problem of generating synthetic earthquakes computationally tractable (Tullis et al., 2012a; Wilson et al., 2018).

The Rate-and-State Earthquake Simulator (RSQsim) was developed by Dieterich and Richards-Dinger (2010) and Richards-Dinger and Dieterich (2012), based on an approach outlined by Dieterich (1995). RSQsim uses static stress transfer between (triangular) fault elements combined with backslip loading (Savage, 1983) to model sequences of synthetic earthquakes. The frictional resistance of these fault elements is determined by a three-regime parameterisation of the earthquake cycle. At a given time step, fault elements are either: 'healing' – locked with shear stress less than the steady-state shear stress, 'nucleating' – accelerating to the (fixed) seismic-slip speed, or 'rupturing' – slipping at the seismic-slip speed until the shear stress again falls below its steady-state value (or slightly below the steady-state value if an optional overshoot is specified). The computational challenge of adapting time-steps to capture both long inter-event times and rapid intra-event rupture propagation is addressed by using the minimum transition time between the three regimes for any fault element in the model as the timestep. The stresses and slip speeds which control these transitions are related by analytical approximations to rate-and-state friction (Richards-Dinger and Dieterich, 2012).

These approximations make RSQsim a computationally efficient approach to generating synthetic earthquake catalogues, which are comparable in duration to paleoseismologically-long time periods (i.e. 100s of thousands to millions of years), for large fault networks. The simulator has several limitations, including assumed constant slip rates (used to calculate loading via a backslip calculation) and emulating, rather than simulating, dynamic stress propagation. However, dynamic models which more accurately capture earthquake physics (e.g. Lapusta et al., 2000; Kaneko et al., 2011; Heinecke et al., 2014; Ando, 2016) cannot yet be used at the temporal and spatial scales of interest for investigating the recurrence of rare earthquakes within country-scale fault systems (Field, 2019), which motivates our use of RSQsim in this study. Both types of model (fully and quasi-dynamic) are subject to uncertainties in fault geometry.

RSQsim has previously been used to inform seismic hazard analysis – perhaps most prominently in California (e.g. Shaw et al., 2018; Milner et al., 2021), as well as to investigate earthquakes on individual faults – including the Alpine fault in A-NZ (Howarth et al., 2021) – and fault systems, such as the Eastern Betic Shear Zone (Herrero-Barbero et al., 2021). The simulator has also been used to investigate appropriate plausibility filters for multi-fault earthquake ruptures in California (Milner et al., 2022) and A-NZ (Gerstenberger et al., 2024a). The California case is somewhat different to A-NZ, because the majority of faults are sub-vertical and strike-slip, meaning that a 2D approach to plausibility filters and fault interactions is often appropriate, whereas in A-NZ interactions at depth are likely to play a significant role in (multi-fault) earthquake kinematics (e.g. Robinson and Benites, 1996; Nicol et al., 2022).

Shaw et al. (2022) constructed the first RSQsim-derived synthetic earthquake catalogue for the whole of A-NZ, using a modified version of the fault model in Stirling et al. (2012). Here we use new fault modelling tools (outlined in section 3.2 below; Howell et al., in review) to develop a fault model based on the New Zealand Community Fault Model (NZCFM; Seebeck et al., 2022, 2023), which represents current expert consensus on the geometries and slip rates of mapped active faults in A-NZ. Our fault model has 3 main improvements to that used by Shaw et al. (2022): 1) using the updated fault geometries now available from Seebeck et al. (2023) as the basis for the fault network, 2) ensuring that faults do not pass through each other at depth, and 3) using a more realistic geometry and slip distribution of the Hikurangi subduction zone (from Williams et al., 2013).

These improvements, and associated effects on the earthquake simulator outputs motivate the construction of a new RSQsim catalogue for central A-NZ.

3.2 3D fault network modelling

We start from the NZCFM map of active fault traces (Seebeck et al., 2022, 2023). We select faults with non-zero slip rates whose traces are either within or intersect our study area (white box in Figure 1, selected faults are shown in black). There are 3 faults which have preferred slip rates of 0 $mmyr^{-1}$ in the NZCFM but which ruptured in the 2016 Kaikōura earthquake (Offshore Splay Thrust, Kowhai and Upper Kowhai - Manakau; Mouslopoulou et al., 2019; Zinke et al., 2019; Howell et al., 2020). We include these faults in our model, and assign them slip rates of 2, 1 and 1 $mmyr^{-1}$ respectively. The preferred slip rate for the Offshore Splay Thrust (OSTF) is 2 ± 1 $mmyr^{-1}$ based on modelling of the uplift of the Kaikōura peninsula (Nicol et al., 2023). The slip rates on the other two faults are unconstrained, so these rates are chosen to allow the faults to rupture but not to dominate local seismic activity. We exclude the North Mernoo Fault System, which accommodates offshore internal deformation of the Pacific Plate (Barnes, 1994).

We then follow the method of Howell et al. (in review) to generate our fault network model. The method consists of the following steps:

1. Identify fault sections in the NZCFM which form part of the same fault or fault system (e.g. Alpine: Kaniere to Springs Junction and Alpine: Springs Junction to Tophouse). Specifying which fault sections are connected allows sections with varying dip and strike to be connected rather than imposing sudden changes in geometry mid-fault, or requiring constant fault dip along strike (as in the model of Shaw et al., 2022).

2. Generate a hierarchy of faults. Faults higher in the hierarchy truncate those lower in the hierarchy if the faults intersect (either at the surface or at depth). This hierarchy is primarily based on fault slip rate (e.g. the Alpine fault truncates the Hope fault), but contains some variations to generate a geologically and geophysically reasonable fault network.

3. Generate depth contours and footprints (the area surrounding each fault's surface projection, as described in Howell et al., in review) for each of the faults.

4. Use the Seequent Ltd software Leapfrog-Geo (Seequent, 2024) to generate surfaces associated with each of the faults, and truncate them against a depth surface. The depth surface we use is the maximum rupture depth based on thermal constraints from Ellis et al. (2021) (their 'Df'). We use this upper bound on seismogenic depths as a limit on the depths to which earthquakes might propagate, but truncate the region where rupture nucleation is likely through tapering the slip rate distributions on faults (see below). Where the Williams et al. (2013) model of the subduction interface is shallower than this seismogenic depth, we use this interface model as the basal surface for the crustal faults.

5. Identify where faults intersect and truncate them appropriately. Leapfrog-Geo creates 3D isosurfaces 500 m from these intersection lines. These isosurfaces are used either to cut slots in a fault surface (if it is partially intersected by a fault higher in the fault hierarchy) or to split a fault surface in two (if the surface is fully bisected by a fault higher in the fault hierarchy). In the latter case, Leapfrog-Geo then determines which section of the split fault surface to keep based on proximity to the mapped surface trace of the fault. We manually check the resulting fault surfaces.

6. Export the resulting 112 fault meshes and remesh them using using Coreform Cubit-2022.11 (used under an educational licence National Technology & Engineering Solutions of Sandia, LLC., 2022). Here we use $\sim$2 km-edged triangles, which are expected to correspond to earthquakes of magnitude $\sim M_w$ 4.3 (using the scaling relations developed by Hanks (2002), which are appropriate for small earthquakes – the A-NZ-specific scaling relationships of Stirling et al. (2023) only apply to earthquakes $\geq M_w 7$).

In one of our models we also include the Hikurangi subduction interface. We model this interface separately to the crustal faults but mesh it at the same resolution and truncate crustal faults against it (effectively placing the subduction interface as the top fault in our hierarchy). We truncate the interface at $\sim$40.3° S, $\sim$100 km outside of our study region. Limiting the extent of the interface in this way means that we do not expect to see full-scale subduction interface ruptures in our synthetic catalogues and may also affect the timing of megathrust ruptures. However, the Hikurangi subduction interface already contributes over 50% of the fault elements to our model, dominating the significant computational resources required to run the earthquake simulator (section 3.3).

Finally, we assign slip rates to the resulting fault meshes based on the preferred slip rates in the NZCFM. The exceptions are the 3 faults discussed above, and the subduction interface, where we use a smoothed version of the coupling model from Wallace et al. (2012), multiplied by the plate convergence rate to generate a non-uniform slip rate across the interface (Figure 2). For the other faults in the model, we identify the closest NZCFM segment to that section of fault (deconstructing combined faults into their original fault segments). We then use univariate splines to taper the slip rate to 0 starting at 2/3 of the depth to the fault base (following Ellis et al., 2021), and 25% of the along strike fault length. We impose a minimum side taper distance of 4 km and a maximum of 10 km to prevent overly large proportions of long faults from being tapered. For combined faults, we imposed the same side tapers but between the slip rates of adjacent sections. For very short faults ($<$10 km)

we set the slip rate on exterior patches to be half of the preferred slip rate. Many of the small faults have triangular or irregular geometries, due to the way they are truncated in the model construction so this tapered-slip approach reduces potential stress concentrations at the fault edges.

Figure 3 shows the distribution of hypocentral depths in each of the models. The histograms for the synthetic catalogues show relatively smooth distributions with depth, suggesting that our tapered slip approach prevents all events from nucleating at the edges of faults, particularly the downdip edge, a challenge for previous RSQsim models (Shaw et al., 2018).

The final fault network, with slip rates, is shown in Figure 2. The fault combinations, hierarchy, mesh files and resulting RSQsim inputs are all available on Zenodo (see Data and Code Availability).

The fault system in A-NZ comprises numerous shallow-to-moderate dipping structures, making it more complex to model than regions with predominantly sub-vertical strike-slip faulting, such as California (e.g. Robinson and Benites, 1996; Robinson, 2004). Our intention is for this network to provide one geologically-reasonable possibility, and a starting point for considering alternative fault network geometries, rather than a definitive model. Indeed, the main motivation behind the development of the semi-automated fault network construction tools in Howell et al. (in review) was to enable more rapid exploration of alternative geometries. Being able to generate such 3D models may be helpful for visualising and understanding some of the implications of, for example, changing the dip of particular fault segments on fault interconnectivity at depth.

Our method does not currently allow for listric faults, so we cannot capture the possibility of crustal faults soling into the plate interface (e.g. Barnes et al., 2002). In addition, RSQsim uses a purely elastic rheology, which means that incorporating the brittle-ductile transition and fault creep is out of scope. In reality, the intersections between faults are likely to be highly complex, and consist of brecciated, deformed rocks with potentially different elastic properties to their surroundings (e.g. Faulkner et al., 2010). Whilst both of these limitations would provide interesting work for future study, for this initial model we use the simpler approach of truncating faults against the subduction interface and each other, without the surfaces being in direct contact.

3.3 Catalogue generation

We use the New Zealand eScience Infrastructure (NeSI) to run two RSQsim simulations, one with and one without the Hikurangi subduction interface. Both simulations were run with a wall time of 168 hours (∼1 week) on 108 cores, with upper model-time limits of 1.42×10^{13} s (∼450 kyr) and maximum 3 $\times10^{10}$ earthquakes (chosen such that the maximum number of earthquakes would not be the limiting factor). The main computational constraint on running these models is RAM. The RAM required scales as the number of patches squared, and is about 160 Gb for the $\sim 10^5$ patches in our model. This high RAM requirement is dominated by a single step in the programme – the calculation of stiffness matrices – so could probably be reduced in future.

We choose the time duration of the synthetic catalogue to be 440 kyr (after removing the first 10 kyr to allow for spin-up effects Hughes et al., 2023) such that we might reasonably expect to see multiple Kaikōura-like events. If we assumed Poissonian recurrence with a rate, λ, of 1 event per 3 kyr (Brough et al., 2023, cf.) then the probability of not observing any such events drops below a probability $P\,(0)$ after time $-\frac{1}{\lambda}\ln P\,(0)$ (e.g. there is less than 1% probability of not observing such events after ∼14 kyr). In order to sample variation in interevent time, we therefore expect to need a catalogue of several hundred thousand years duration (although we note that this approach is an approximation – neither the synthetic earthquakes, nor observed earthquakes, are likely to be strictly Poissonian, since their occurrence is dependent on that of previous events, e.g. Gerstenberger et al., 2024b; Iturrieta et al., 2024).

We use uniform frictional parameters throughout the model, with $a-b$ =-0.005. This value is consistent with previous studies using RSQsim in Aotearoa-New Zealand; the earlier studies of Shaw et al. (2022) and Hughes et al. (2023) used $a-b$ =-0.007, but more recent studies such as Delogkos et al. (2023) and Hughes et al. (2024) have used $a-b$ = -0.003, which Delogkos et al. (2023) found optimised their model fit to the magnitude-area scaling relationships proposed by Stirling et al. (2023). Liao et al. (2024) used values from -5×10^{-4} to -0.003. We find good agreement between our model and previously proposed scaling relations (Figure 4 Hanks, 2002; Stirling et al., 2023), suggesting that the parameters we use are reasonable. Whilst the frictional properties of the fault network are likely to be heterogeneous (e.g. Boulton et al., 2018; Eberhart-Phillips et al., 2021; Brideau et al., 2022), in the absence of further constraints we choose not to introduce additional complexity into our model. By default RSQsim reduces a on all patches in the model domain once an earthquake starts to a factor, f, times a, (here $f = 0.1$, such that $a-b$ will locally drop to -0.014), which helps to emulate the dynamic properties of fault rupture within a quasi-static framework. We limit the range of influence of each patch by specifying the patches within 7.5 km (∼2 patches) in a 'neighbour' file. Tests using immediately adjacent neighbours only effectively prohibit stress transfer between faults but we find larger distances do not have a significant impact on our results. The full specification of parameters used in our model is available, with the results and fault network, on Zenodo (see Data and Code Availability).

3.4 Defining multi-fault earthquakes

Observationally, identifying an earthquake as 'multi-fault' is (relatively) simple; a multi-fault earthquake is one involving either surface rupture on multiple separate active faults, as in Kaikōura 2016 (e.g. Nicol et al., 2023) or a resolvable need for multiple faults at depth to reproduce seismological or geodetic observations, as in

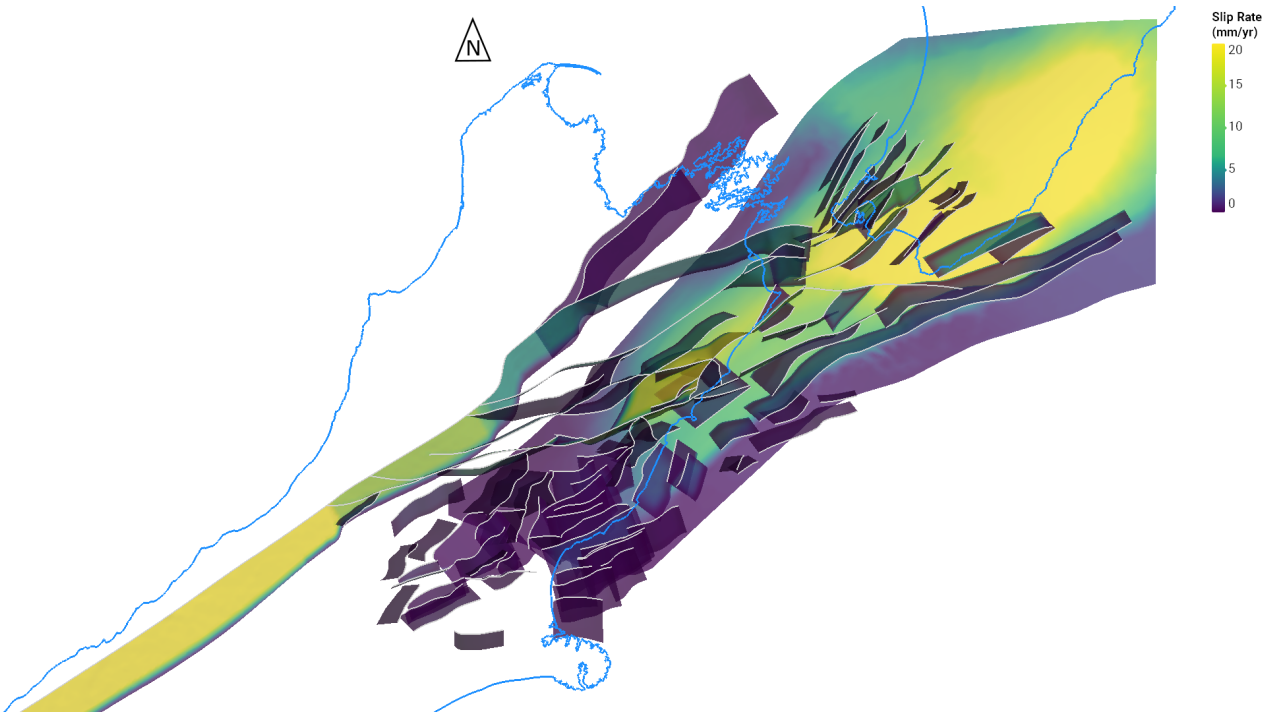

Figure 2 3D fault model of Central A-NZ coloured by slip rate. The study area is shown by the box in Figure 1.

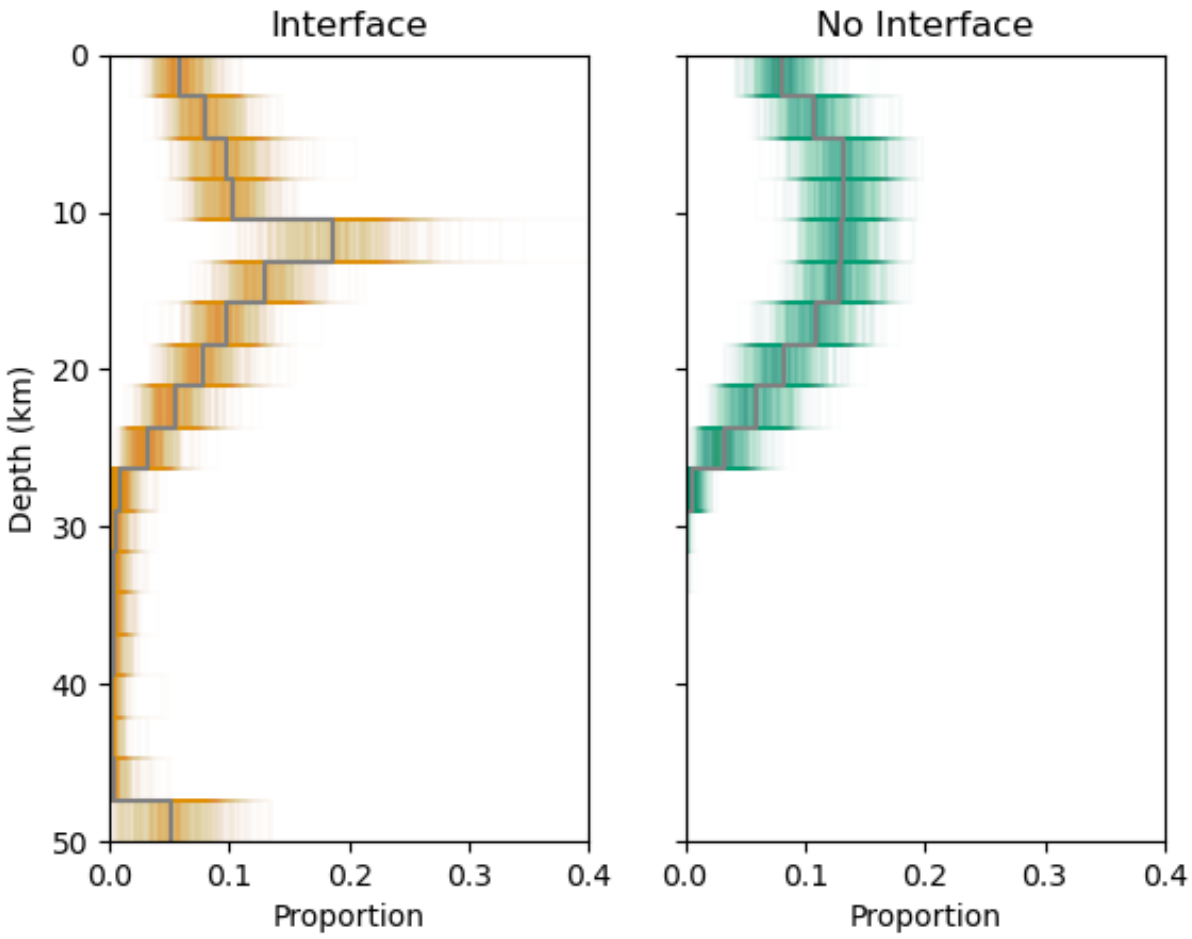

Figure 3 Depth histograms for RSQsim catalogues (left - with the subduction interface, right - without the subduction interface). Coloured lines show depths from 1000 80 year time windows in each catalogue, grey lines show the whole catalogue.

the 2010 Darfield earthquake (e.g. Beavan et al., 2012). However, the appropriate criteria to use for identifying multi-fault earthquakes from an earthquake simulator to compare to these observations are less clear. For simulated earthquakes, we have perfect knowledge of which parts of a fault have moved, and by how much, but these would not necessarily be detectable in observational datasets.

We therefore consider 4 possible definitions of a synthetic multi-fault earthquake:

1. any slip on more than one fault,
2. More than one fault has an effective magnitude release equivalent to $>$M$_w$ 6.
3. Surface rupture on more than one fault (minimum slip of 0.1 m on at least one patch within 1 km of the surface). This definition corresponds to the common observational criteria that multi-fault earthquakes have surface rupture on more than one fault, although the specific definition of surface slip used here ($>$0.1 m in the top 1 km) could well be too small to be detectable paleoseismologically (e.g. Nicol et al., 2016; Coffey et al., 2022). In this definition there is no minimum magnitude release per fault.
4. Surface rupture on more than one fault *and* more than one fault has an effective magnitude release equivalent to $>$M$_w$ 6.

To investigate different definitions we use the effective moment release on the jth fault, $M_{0,j}$;

$$M_{0,j} = \sum_i \mu u_i A_i, \tag{1}$$

where μ, the shear modulus, is 30 GPa, and u_i and A_i are the slip and area of the ith patch on the fault respectively. The effective magnitude release on the jth fault, $M_{w,j}$, is then given by:

$$M_{w,j} = \frac{2}{3}\log_{10} M_{0,j} - 6.03 \tag{2}$$

after Hanks and Kanamori (1979) (converted to Nm).

To capture key features of the 2016 Kaikōura earthquake, without requiring the same faults to be involved, we define complex multi-fault synthetic earthquakes as events with M$_w$ $>$7.5, involving $\geq$ 4 faults with effective magnitude release within 1.5 magnitude units of the effective magnitude released by the principal fault (fault with the highest effective magnitude release). Hamling et al. (2017) used finite fault inversion to model slip on 6 faults (though some of these are combinations of mapped faults e.g. The Humps and Hunderlee and Kekerengu - Jorden - Upper Kowhai) and found the highest effective magnitude release of M$_w$ 7.7 on the Kekerengu - Jorden - Upper Kowhai, with the smallest effective magnitude on the London Hill fault (M$_w$ 6.8) still within one magnitude unit. Similarly, Xu et al. (2018) used 6 faults in their finite fault model and found that all released an equivalent magnitude $\geq$M$_w$ 6.27, with the highest equivalent magnitude release being M$_w$ 7.77 on the Jordan-Kekerengu-Needles fault. We do not constrain these complex multi-fault synthetic earthquakes to be surface rupturing because, whilst surface rupture of multiple faults was clearly a defining feature of the Kaikōura earthquake, surface slip is not necessarily required to generate a destructive, resolvably multi-fault earthquake. The 2010 Darfield earthquake, which occurred 6 years earlier about 150 km to the south-west of the Kaikōura epicentre also involved multiple faults, but in that case the faults predominantly had no surface expression and were mostly inferred from geodetic and seismological observations (Beavan et al., 2010, 2012).

Finally, we define 'Kaikōura-like' synthetic earthquakes as the subset of these complex multi-fault earthquakes which have moment release equivalent to at least M$_w$7 on the Jordan-Kekerengu-Needles fault, in line with e.g. Hamling et al. (2017) and Xu et al. (2018).

4 Results

We briefly describe the overall properties and scaling relationships of our synthetic earthquake catalogues (section 4.1) before looking specifically at the occurrence of multi-fault and 'Kaikōura-like' synthetic earthquakes (section 4.2).

4.1 Synthetic earthquake catalogues

The 'Interface' catalogue contains 8,742,825 synthetic earthquakes between M$_w$ 2.8 and 8.7 and the 'No Interface' catalogue contains 6,481,585 synthetic earthquakes between M$_w$ 2.8 and 8.1 (Figure 4). The subduction interface contributes about half (58%) of the moment rate in the 'Interface' catalogue, which is consistent with the lower productivity of the 'No Interface' catalogue.

Figure 4 shows the magnitude-frequency (top panels) and magnitude-area (bottom panels) distributions for each of these catalogues. We extract the magnitude frequency distribution for the entire catalogue, and for 1000 80-year time samples, for comparison with the instrumental record (which spans ~1940–2020; Rollins et al., 2024). For both catalogues, the magnitude-frequency distributions are consistent with the instrumental catalogue (and Gutenberg-Richter relationships) between ~M$_w$ 5.5 and 7.8 (the maximum magnitude in the instrumental catalogue). The full (unsampled) synthetic catalogues suggest a slightly more characteristic (lower gradient) region between ~M$_w$ 6 and 7, which has been observed in other RSQsim catalogues (e.g. Shaw et al., 2022; Delogkos et al., 2023) and may be related to the specific fault geometries in the model (Delogkos et al., 2023) or to using a homogeneous initial stress state (Liao et al., 2024). The major difference in magnitude-frequency distribution between the 'Interface' and 'No Interface' catalogues is the maximum magnitude, which is M$_w$ 8.7 for the 'Interface' catalogue and M$_w$ 8.1 in the 'No Interface' catalogue. This difference is consistent with the subduction interface being involved in the largest earthquakes (Stirling et al., 2012; Gerstenberger et al., 2024a).

Both catalogues also show reasonable agreement with the magnitude-area scaling relations for A-NZ for

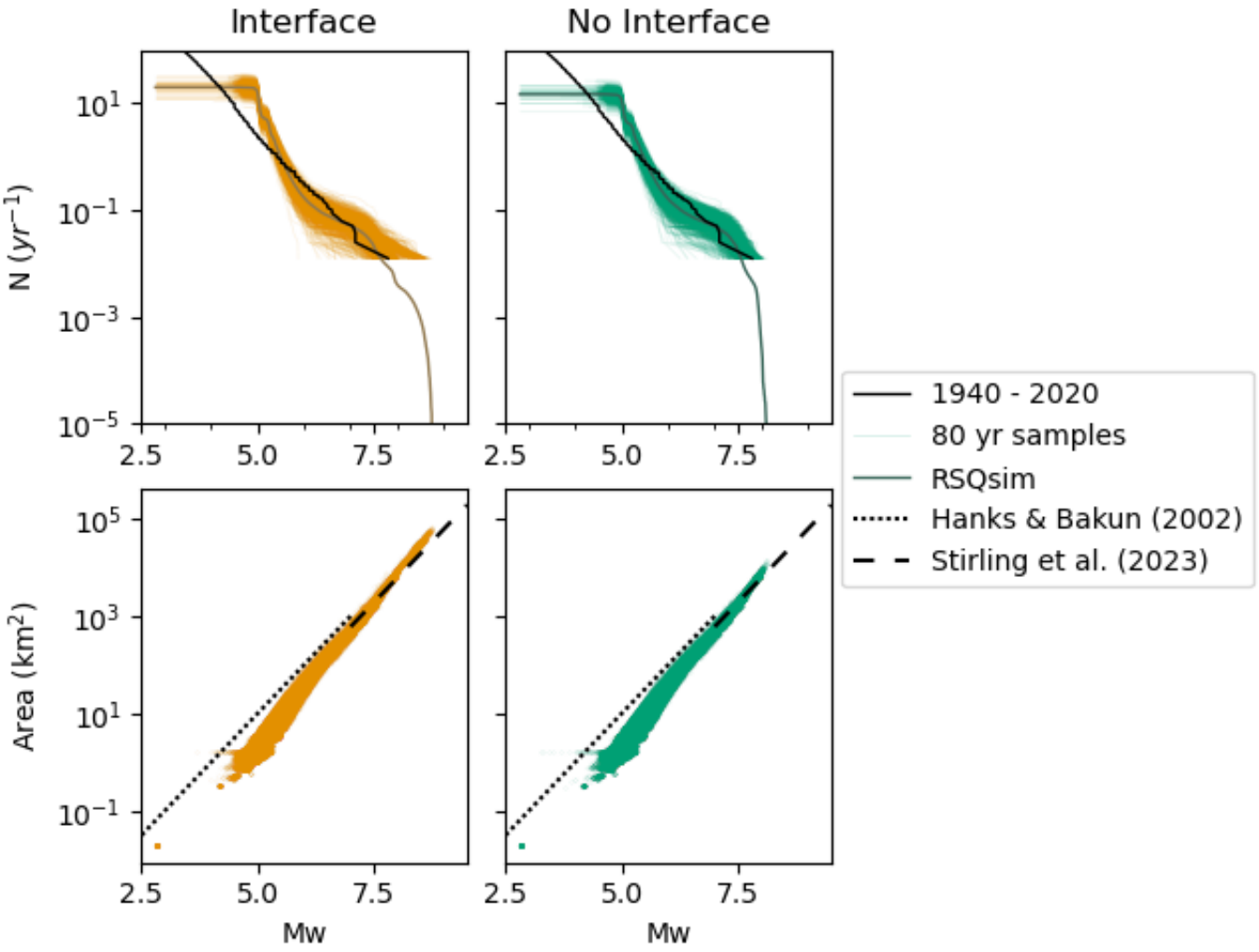

Figure 4 Scaling relationships for RSQsim catalogues (left - with the subduction interface, right - without the subduction interface). Top panels show magnitude-frequency distributions for 80 year samples from these catalogues (bright colours) and the whole catalogue (darker colours). The instrumental record, from Rollins et al. (2024), is plotted in black. Bottom panels show the magnitude - area scaling for events in each catalogue. Dotted black line is the scaling relationship proposed by Hanks (2002), and dashed black line is that proposed by Stirling et al. (2023), for M_w >8 and used in the New Zealand National Seismic Hazard Model 2022 (Gerstenberger et al., 2024a).

earthquakes $\geq$M$_w$7 (Stirling et al., 2023). Figures 4c and d show this scaling relationship (dashed lines) and those of Hanks (2002), which extends to smaller magnitudes. Stirling et al. (2023)'s relationship is a better fit to the simulator results, particularly at the high magnitudes for which it was developed. Smaller areas at low magnitudes ($<\sim$M$_w$4.5) are likely related to the minimum rupture area of an earthquake in the model being set by the patch size. Smaller events can either occur on smaller patches (we set the target patch dimensions, rather than the specific patch dimensions; section 3.2) or with reduced slip. Synthetic earthquakes from M$_w$4 – 4.2 therefore have constant area but reduced slip.

Consistency of the synthetic catalogues with observed scaling relations suggests that the synthetic catalogues are a reasonable model of earthquakes in the Central A-NZ region, though more detailed and particularly more quantitative testing is important before such catalogues are used for hazard assessment.

4.2 Multi-fault synthetic earthquakes

4.2.1 Proportion of multi-fault synthetic earthquakes

The proportion of multi-fault synthetic earthquakes increases with minimum magnitude for all definitions of 'multi-fault' (section 3.4, Figure 5a and b). Almost all synthetic earthquakes $> M_w \sim 8$ have slip on patches on more than one fault (definition 1 in section 3.4, blue in Figure 5) for both the 'Interface' and 'No Interface' catalogues (97 and 99% respectively, with only 1 earthquake >M$_w$ 8 in the 'No Interface' catalogue which occurs on a single fault). This result is consistent with a decreasing proportion of faults being capable of hosting larger magnitude synthetic earthquakes individually (since RSQsim effectively reproduces magnitude-area scaling relationships, section 4.1).

Definitions 2 and 3 (synthetic earthquakes with greater than M$_w$ 6 effective magnitude release on more than one fault, yellow in Figure 5; synthetic earthquakes with surface slip on more than one fault, green in Fig-

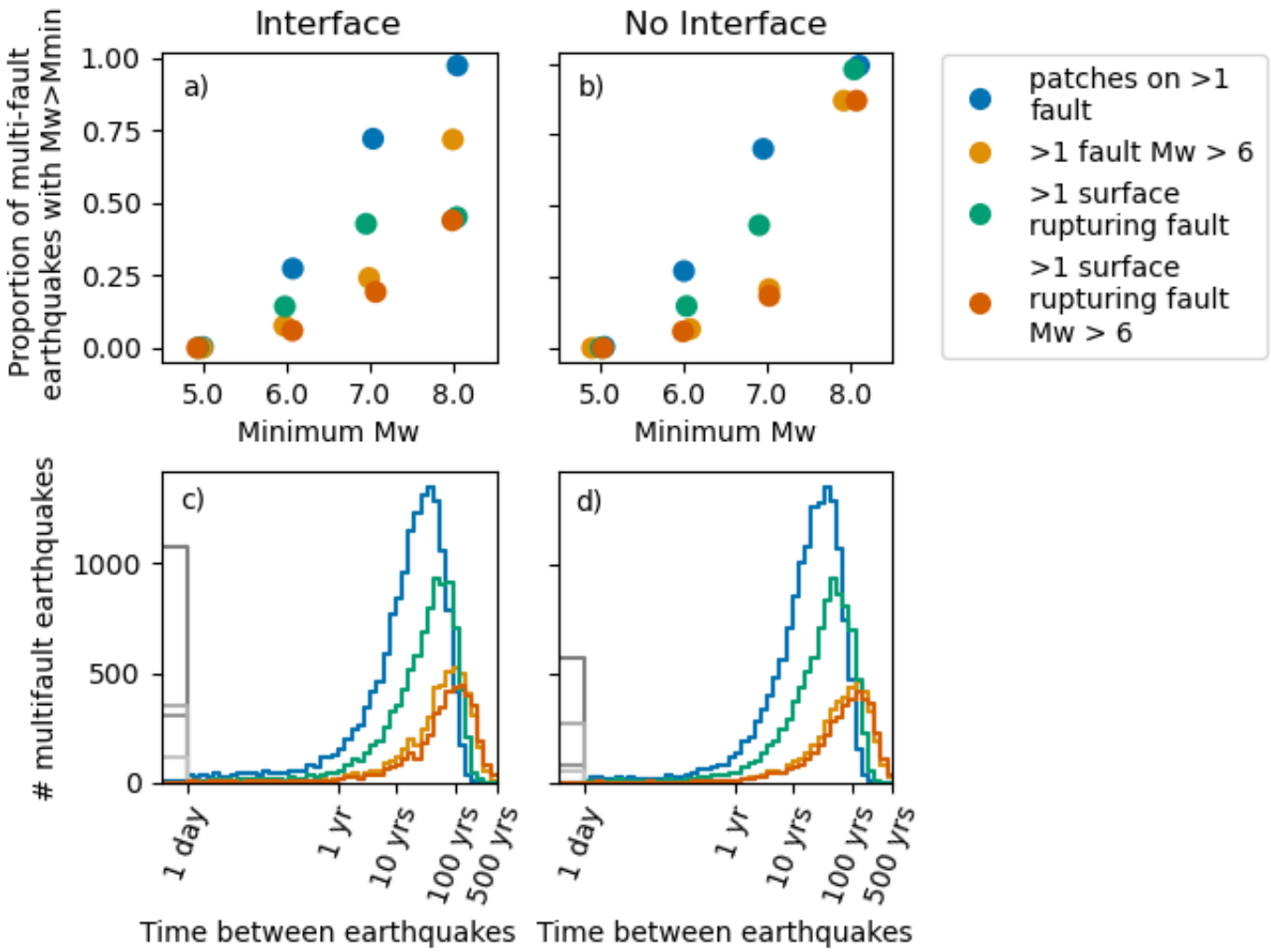

Figure 5 Effects of choosing different definitions of 'multi-fault' on the proportion of multi-fault earthquakes in catalogues with (left panels) and without (right) the subduction interface. Top panels show the proportion of multi-fault earthquakes with $M_w > M_w^{min}$ using different definitions. Bottom panels show histograms of the times between multi-fault events with M_w>7 using these different definitions.

ure 5) are subsets of those with slip on patches on more than one fault (definition 1). As such the proportions of earthquakes meeting these definitions of 'multi-fault' are lower at all magnitudes than our first definition (though for the 'No Interface' there is very little difference between definitions 1 and 3 i.e. most earthquakes with slip on multiple faults also have surface slip on multiple faults). The final potential definition of multi-fault we use here – surface rupture on more than one fault and more than one fault having an effective magnitude release equivalent to $>M_w$ 6 (definition 4 in section 3.4, orange in Figure 5) – is a subset of all of the other definitions, so has the lowest proportion of synthetic earthquakes at all magnitudes. However, this definition is most likely to be detectable observationally, suggesting that the proportion of earthquakes rupturing multiple faults may be larger than we are able to observe geologically or geodetically.

The relatively small proportion of surface rupturing multi-fault earthquakes in the 'Interface' catalogue reflects that larger magnitude events in this catalogue mostly involve the Hikurangi subduction interface, which is not considered to host surface ruptures in our model because its trace is buried (Barnes and De Lépinay, 1997). In contrast, in the 'No Interface' catalogue the majority of earthquakes rupturing patches on more than one fault also have surface rupture at higher magnitudes (slip across the full fault surface is required to produce the maximum magnitudes in the catalogue, e.g. 99% of earthquakes $>M_w$8 involve more than 1 fault and 98% of these earthquakes are surface rupturing).

4.2.2 Recurrence intervals of multi-fault synthetic earthquakes

Figure 5c and d show the time between multi-fault synthetic earthquakes with M_w >7 using each of the definitions in section 3.4. We focus on two key results from Figure 5c and d: first, that how we define a multi-fault earthquake affects the time between similar earthquakes and second, that a significant number of synthetic multi-fault earthquakes occur less than one day apart.

The time between similar synthetic earthquakes is shortest for our least restrictive definition of a multi-fault earthquake (definition 1 in section 3.4 – slip on patches on more than one fault). Requiring surface rup-

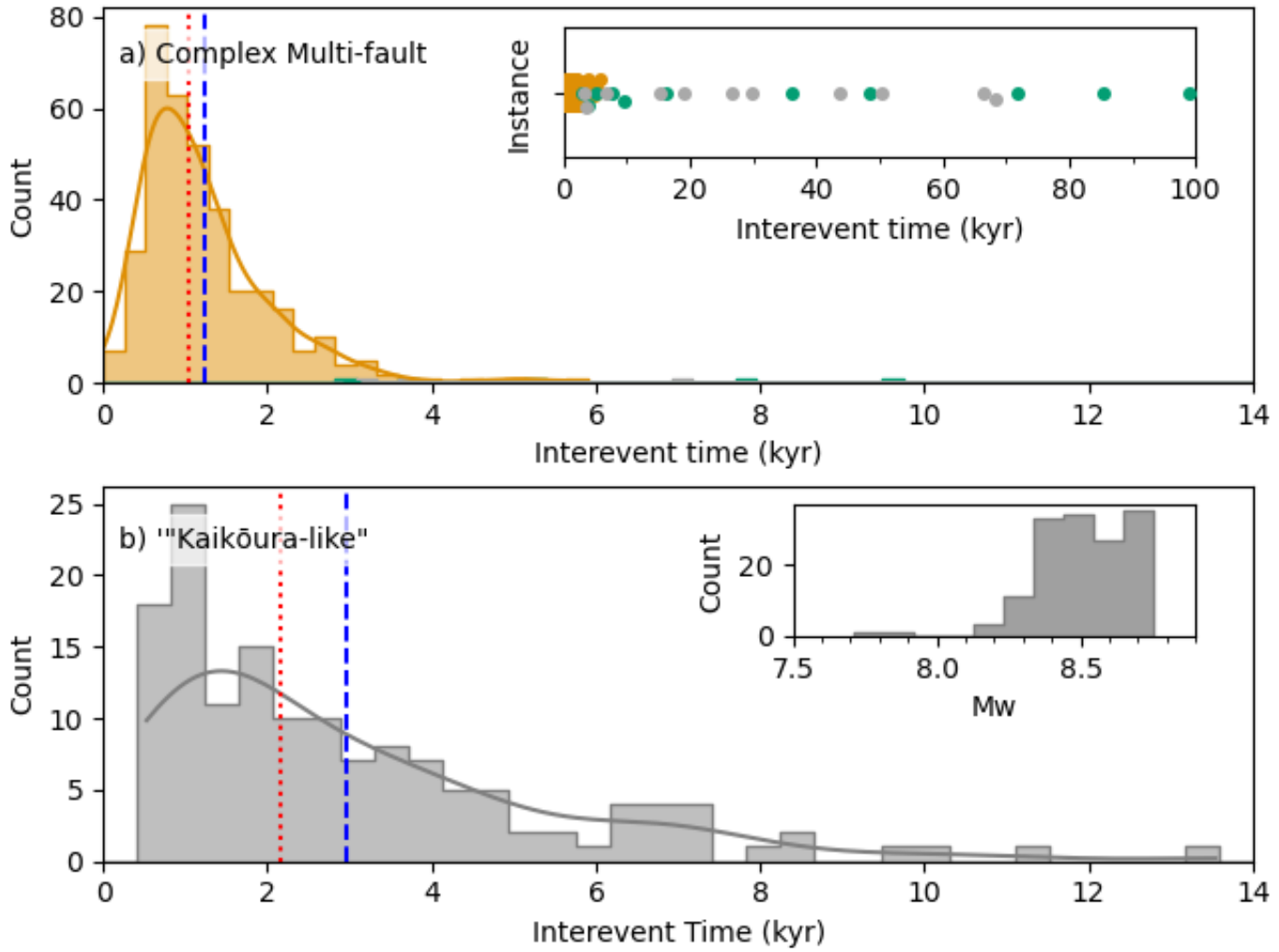

Figure 6 Interevent times for a) complex multi-fault synthetic earthquakes(M_w >7.5, involving ≥ 4 faults within 1.5 magnitude units of the highest moment release fault, section 3.4, defined to capture key features of the Kaikōura earthquake). Counts are dominated by earthquakes which involve the subduction interface (n=357, orange histogram and kernel density estimate plot) which have a mean interevent time of 1.2kyr and a coefficient of variation of 0.66. Complex multi-fault events which involve only crustal faults are shown in green ('Interface' catalogue) and grey ('No Interface' catalogue). Inset panel shows the time between events of each type for longer interevent times (up to 100 kyr), which are typically for events not involving the subduction interface, whereas the maximum interevent time for a complex multi-fault earthquake involving the subduction interface is ∼6 kyr. Note that because these plots are for a class of earthquakes, not events on a particular fault, the interevent times are not directly comparable to paleoseismic interevent times on a single fault.b) shows the interevent time distribution for the subset of complex multi-fault event which have moment release equivalent to at least M_w7 on the Jordan-Kekerengu-Needles (JKN) fault, which we term 'Kaikōura-like'. The inset shows the distribution of magnitudes for such 'Kaikōura-like' earthquakes. Blue and red lines in a) and b) show the mean and median interevent times respectively.

ture on more than one fault (definition 2 in section 3.4) increases the median time between multi-fault earthquakes by ∼50% from 21 (22) to 36 (37) years (values in brackets refer to the 'No Interface' catalogue) and reduces the number of events (unsurprisingly, since this criterion is a subset of definition 1). A more significant effect is seen from introducing the requirement of at least one fault having an effective magnitude release greater than M_w 6 (orange and yellow lines in Figure 5). The median time between multi-fault synthetic earthquakes then increases to 67 (76) and 81 (87) years for definitions 3 and 4 (section 3.4) respectively, a factor of 4 increase over definition 1, where the values in brackets refer to the 'No Interface' catalogue. Introducing the additional surface-rupturing criterion (definition 4 in section 3.4) has a small effect for the 'Interface catalogue', due to the Hikurangi subduction zone not generating surface ruptures in the model (section 3.4), but negligible effect on the distribution of times between events for the 'No Interface' catalogue. The small size of this effect shows that the majority of synthetic earthquakes with effective magnitude release >M_w6 on more than one fault are surface rupturing.

The grey bars in Figure 5c and d show times between synthetic multi-fault earthquakes less than one day. There are >1000 of these in the 'Interface' catalogue and >500 in the 'No Interface' catalogue. Even allowing for the larger number of synthetic earthquakes in the 'Interface' catalogue, these short times between events are much more common when the subduction inter-

face is included in the model. These short interevent times are related to the definition of an earthquake in RSQsim (section 5.1). We have therefore removed synthetic multi-fault earthquakes less than one day apart in calculating the median times between synthetic earthquakes quoted in the paragraph above (although we note that they have little effect, e.g. the median recurrence intervals for synthetic multi-fault earthquakes using definition 4 in the 'Interface' and 'No Interface' are 79 and 85 years including these closely-spaced synthetic earthquakes, and 81 and 87 years respectively without).

Figure 6a) shows the time between complex multi-fault earthquakes in the synthetic catalogues. The mean interevent time for complex multi-fault synthetic earthquakes involving the subduction interface is 1200 year, with a coefficient of variation of 0.66. Note that these interevent times are not the time between events on a particular fault, so are not directly comparable to paleoseismic interevent times or recurrence intervals. There are only 12 complex multi-fault earthquakes in each catalogue which do not involve the subduction interface. The times between these events are shown in the inset of Figure 6a) - there are not enough of these synthetic earthquakes to assess the statistical properties of their temporal distribution but the interevent times are much longer (of order 10s kyr) than those involving the subduction interface.

Both the fault which releases the majority of the seismic moment and the fault on which the earthquake initiates are dominated by the Hikurangi subduction interface for these complex multi-fault events. The mean interevent times for complex multi-fault events with the dominant moment release on the Hikurangi is 1250 yrs, with a coefficient of variation of 0.65, similar to the mean interevent times of all complex multi-fault earthquakes in the catalogue. Events with the dominant moment release on the Alpine or Wairarapa faults are less frequent and have longer ($\geq$10 kyr), less periodic interevent times. There are a few instances of the times between complex multi-fault earthquakes initiating on the Wairarapa fault being $<$5 kyr, but for most faults other than the Hikurangi the times between complex multi-fault earthquakes are $>$ 10 kyr and there are too few such events to identify statistical trends.

4.2.3 Fault co-ruptures and aspect ratios of synthetic multi-fault earthquakes

Another way to think about multi-fault earthquakes is in terms of which faults co-rupture. Figure 7 shows the number of synthetic earthquakes with M_w $>$6.5 which co-rupture high slip-rate faults in our model for the 'Interface' (a) and 'No Interface' (b) catalogues. The 12 fastest crustal faults are ordered on each axis by their maximum slip rate (from Jordan-Kekerengu-Needles, with the highest slip rate in the model, to Clarence). On-diagonal elements represent the number of single-fault synthetic earthquakes on that fault, whilst off-diagonal elements represent the number of times the two associated faults co-rupture. Figure 7c shows the difference in the number of synthetic earthquakes in each category between the two catalogues, with red squares showing co-ruptures which occur more frequently in the 'Interface' catalogue and blue squares showing co-ruptures which occur more frequently in the 'No Interface' catalogue.

For both catalogues, the two highest slip rate faults (Jordan-Kekerengu-Needles and the Hope fault) have the largest numbers of single-fault earthquakes. However, for lower slip-rate faults the picture becomes more complicated, with variable proportions of single- and multi-fault synthetic earthquakes, suggesting that slip-rate is not the key control on multi-fault rupture in RSQsim. Some illustrative examples are: 1) the Hope-Hanmer NW fault (Figure 8f), 2) the Wairarapa and Wellington Hutt Valley faults (Figures 8j and k) and 3) the Booboo and Jordan-Kekerengu-Needles faults (Figures 8c and g).

Hope-Hanmer NW is a short fault bounding the northwestern edge of the Hanmer basin which connects parts of the Hope fault (e.g. Wood et al., 1994). The diagonal elements of Figure 7a and b show that the Hope-Hanmer fault is not involved in any single-fault synthetic earthquakes in either of our catalogues. Instead, the fault co-ruptures primarily with the Hope fault, and the Kākāpō fault, which branches off the Hope fault slightly SW of the Hanmer basin. The prevalence of these co-ruptures is consistent with the A-NZ National Seismic Hazard Model (Gerstenberger et al., 2024a), where ruptures of the Hope-Hanmer NW with a return period $<$1 Myr all involve adjacent segments of the Hope fault. These co-ruptures are also consistent with the geometry of the Hope-Hanmer NW, which is very close to these adjacent faults (e.g. the Hope and Kākāpō faults) , so likely to easily transfer stress from and to these adjacent faults segments.

The Wairarapa and Wellington Hutt Valley (WHV) faults both have over 500 single-fault synthetic earthquakes with M_w $>$6.5. Both, however, are also involved in a significant number of multi-fault earthquakes, with co-ruptures of the WHV and Wairarapa fault dominating for the WHV in both catalogues, and for the Wairarapa in the 'Interface' catalogue. The other faults which co-rupture with these two faults are strongly affected by the presence or absence of the subduction interface, which we discuss further below. Interaction of these two faults is very important for the seismic hazard posed to Wellington (A-NZ's capital city), and has been discussed in the context of interpreting paleoseismic records from the lower North Island (e.g. Humphrey et al., 2025). The Wairarapa fault in particular has also been discussed as having potential connectivity to faults across the Cook Strait (Grapes and Holdgate, 2014), such as the Awatere fault (the Awatere-Vernon fault in our model), which we see in both the 'Interface' and 'No Interface' catalogues.

The Boo Boo fault (Figure 8c) is an offshore, steeply-dipping right-lateral fault striking sub-parallel to the plate motion direction (Barnes and Audru, 1999a,b; Wallace et al., 2012). Wallace et al. (2012) noted the geometrical connectivity of this fault and the adjacent Kekerengu (to the SW) and Wairarapa (to the N) faults, and suggested that this geometrical connectivity might also lead to a kinematic connection. In our mod-

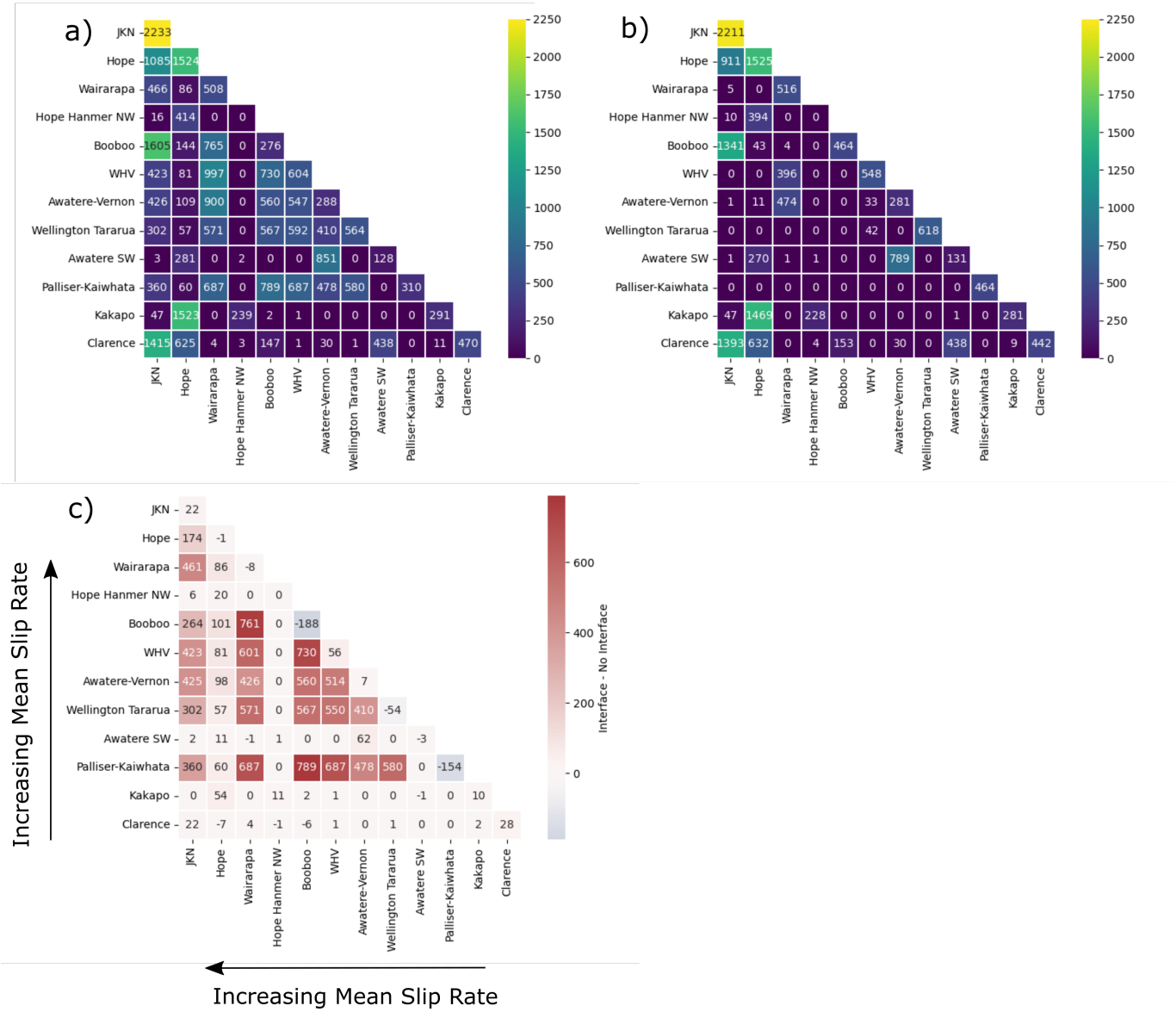

Figure 7 Occurrences of co-ruptures on high slip rate faults. a) and b) show the number of co-ruptures of faults in the 'Interface' and 'No Interface' models, respectively. Diagonal squares show the number of single fault earthquakes on each fault. Catalogues are filtered to synthetic earthquakes with M_w>6.5. Note that because some earthquakes involve more than two faults, the sum of the numbers across the whole heat map is greater than the total number of synthetic earthquakes with M_w >6.5 in each catalogue. c) shows the difference in the number of co-ruptures between these two models ('Interface'-'No Interface', i.e. a)-b)). The diagonal squares show the change in the number of single-fault earthquakes on that fault between the two models.

els, the Boo Boo fault dominantly ruptures with the Jordan-Kekerengu-Needles fault (we note that there is some complexity in a direct comparison to the behaviour of the Jordan, Kekerengu and Needles faults since the three form a continuous along-strike structure in our model, section 3), which is consistent with the idea of kinematic along-strike connectivity. However, co-ruptures with the Wairarapa fault, which is across strike, though in very close surface-proximity to the Boo Boo fault at its SW end, occur much more frequently in the 'Interface' catalogue.

Figure 7c shows that there are substantial differences in which faults (co-)rupture between the 'Interface' and 'No Interface' catalogues. Figure 8 shows the same information in map-form for the nine highest slip-rate crustal faults, here normalised by the maximum difference between the two catalogues for each primary fault. This map view shows that the main difference between the two catalogues is the increased prevalence of co-ruptures with faults located across-strike from the primary fault in the 'Interface' catalogue, particularly where these faults are above the shallow part of the subduction interface (the black dashed line in each panel shows the 30 km depth contour for the subduction interface from Williams et al., 2013). For example, the Boo Boo and Wellington Hutt Valley faults co-rupture 765 times in the 'Interface' catalogue, and only 4 in the 'No Interface' catalogue. The Wairarapa fault is also an illustrative example. This fault co-ruptures much more frequently with both across- (e.g. Boo Boo, Palliser-Kaiwhata) and along-strike (e.g. Awatere-Vernon) faults in the 'Interface' than the 'No Interface' catalogue. The

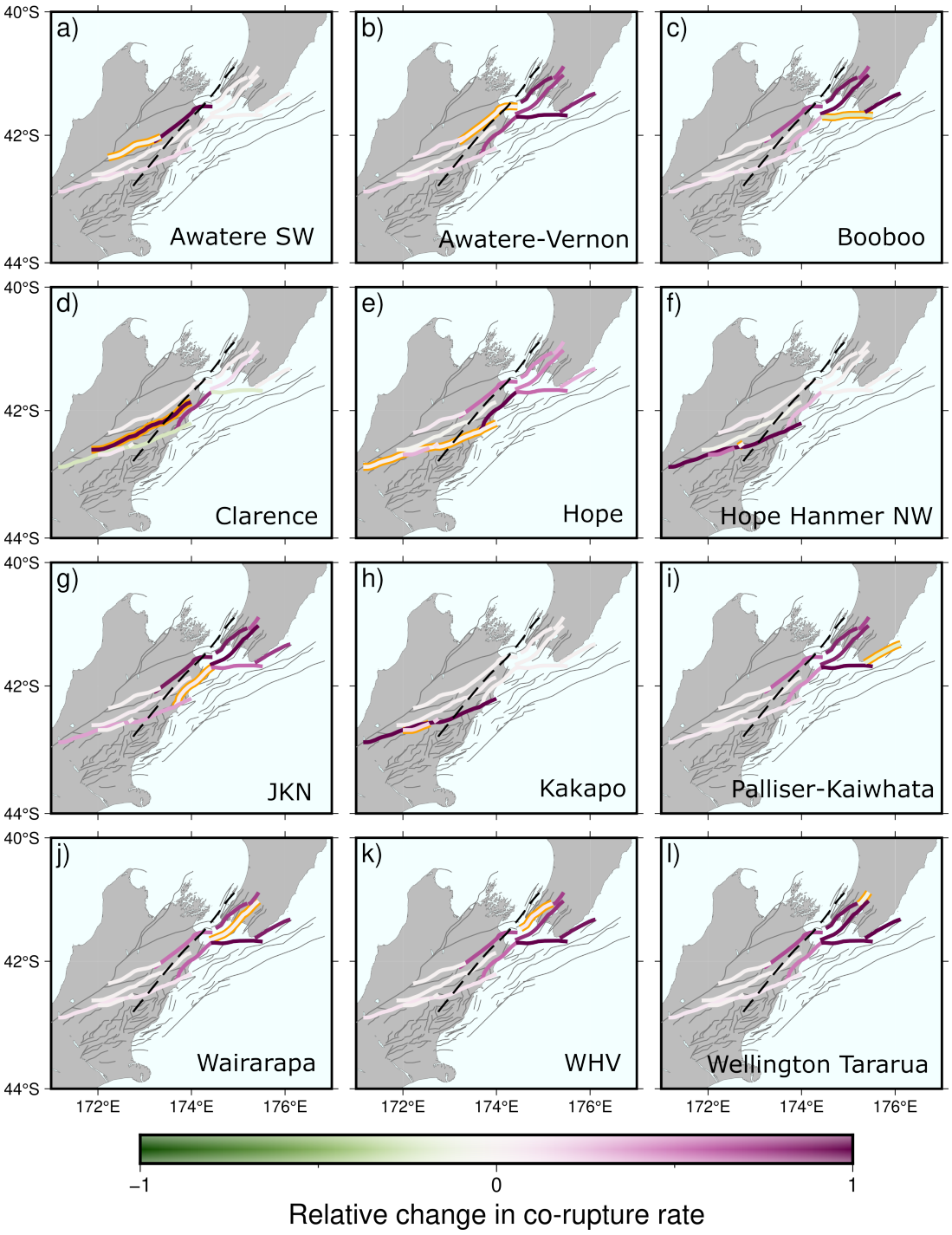

Figure 8 Relative occurrence of co-ruptures on high slip rate faults between our two simulations. This figure is a geographical representation of the information in figure 7. The rate is the normalised difference ('Interface'-'No Interface' / maximum difference for that primary fault) in the number of synthetic earthquakes involving both the primary fault (highlighted in orange) and each other fault. Purple colours imply more events rupture both that fault and the primary fault in the 'Interface' than the 'No Interface' model. The colour of the primary fault reflects the change in single fault ruptures on that fault. Dashed line shows the 30km contour from the interface model of Williams et al. (2013) – we expect this contour to form an approximate dividing line with crustal faults up-dip (South-East) of this line interacting with the interface, whilst those to the North-West do not. Primary faults: a) Awatere South West, b) Awatere-Vernon, c) Boo Boo, d) Clarence, e) Hope, f) Hope Hanmer North West, g) Jordan-Kekerengu-Needles, h) Kakapo, i) Palliser-Kaiwhata, j) Wairarapa, k) Wellington Hutt Valley, l) Wellington Tararua.

suggestion that the Wairarapa fault might co-rupture with across-strike faults is consistent with recent paleoseismological evidence (Humphrey et al., 2025). Similarly, the Palliser-Kaiwhata fault, which is located in the offshore Hikurangi accretionary prism, has only single-fault ruptures in the 'No Interface' catalogue, but predominantly co-ruptures with across-strike faults in the 'Interface' catalogue.

Our findings from fault co-ruptures are supported by the aspect ratios of synthetic earthquakes in the two cat-

alogues. We define the aspect ratio of a synthetic earthquake as the ratio between its across-strike length (furthest map distance between patches on crustal faults which rupture taken perpendicular to the mean strike of the earthquake) and its along-strike length (furthest map distance between patches on crustal faults which rupture, taken parallel to the mean strike of the earthquake). Aspect ratios less than 1 (Figure 9) therefore represent ruptures which are longer than they are wide, which we might expect for earthquakes on steeply dipping faults or, in the case of multi-fault earthquakes, if the faults which co-rupture are along strike from each other. Higher aspect ratios would be expected either for more shallow dipping faults, or if a multi-fault earthquake ruptures faults which are across strike from each other – a scenario not normally permitted by plausibility filters for steeply-dipping faults (e.g. Milner et al., 2013, 2022; Gerstenberger et al., 2024a). Note that we exclude the subduction interface from the aspect ratios to make an appropriate comparison between aspect ratios of crustal faulting in our two synthetic earthquake catalogues.

For all synthetic earthquakes with M_w>6.2 (equivalent to the moment release from two magnitude 6 earthquakes to ensure the comparison to multi-fault earthquakes is representative) we see similar trends in both the 'Interface' and 'No Interface' catalogues (Figure 9), with a positive skew and dominantly low-aspect ratio ruptures. However, for multi-fault earthquakes (using the definition of multiple faults having M_w6 or greater equivalent moment release) we see the there is a broader tail to the aspect ratios of synthetic earthquakes from the 'Interface' catalogue, that is, there are more events with higher aspect ratios in the 'Interface' catalogue. This broad tail is consistent with the increased prevalence of co-ruptures between across strike faults shown in figures 7 and 8, and suggests that the subduction interface may act as a linking structure facilitating stress transfer at depth.

4.3 Kaikōura-like synthetic earthquakes

In section 3.4 we defined 'Kaikōura-like' earthquakes complex multi-fault synthetic earthquakes which have moment release equivalent to at least M_w7 on the Jordan-Kekerengu-Needles fault. Figure 6b) shows the distribution of interevent times and magnitudes (inset) for these events. The mean interevent time for 'Kaikōura-like' events is ∼3000 yrs, with a coefficient of variation of 0.82. The interevent time distribution is positively skewed, however, so the median value (2150 yrs) provides a better measure of the distribution. A positive skew to the interevent times is consistent with Poissonian event occurrence (most earthquakes have relatively short times between them but there is sometimes a break of over 10 kyr), although further work is required to understand how, or whether, this property of the simulated earthquakes relates to actual Kaikōura-like events.

Although we require these 'Kaikōura-like' events to have an equivalent moment release of M_w 7 on the Jordan-Kekerengu-Needles fault, the Jordan-Kekerengu-Needles fault is neither the initial fault nor – in contrast to the 2016 Kaikōura earthquake – the fault with the largest moment release for these events. Rather, the Hikurangi subduction interface, whose role in the 2016 earthquake remains debated (section 2), dominates the moment release for all but 2 'Kaikōura-like' events in the 'Interface' catalogue (Figure 10a, b, c). Similarly, there are only 2 such events in the 'No Interface' catalogue (Figure 10 d, e), emphasising the role of the subduction interface in 'Kaikōura-like' multi-fault events.

5 Discussion

We have presented the first use of the 3D fault modelling techniques described by Howell et al. (in review) in an earthquake simulator. These new modelling techniques allow us to generate a fault model for central A-NZ which is more consistent with both mapped faults in the region (Seebeck et al., 2023) and geological understanding of the interaction of faults at depth than previous simulations. We now discuss our initial findings from these simulations in the context of the three key questions outlined in section 1, namely: 1) how common are multi-fault ruptures? 2) Can RSQsim produce synthetic earthquakes with similar properties to the 2016 Kaikōura earthquake (section 2)? and 3) what is the role of the Hikurangi subduction interface in controlling the proportion of earthquakes which are multi-fault and the recurrence interval, magnitude and geometry of such earthquakes? We also suggest potential avenues for future research.

5.1 How common are synthetic multi-fault earthquakes?

Faults in our synthetic catalogues rupture in both multi-fault and single fault synthetic earthquakes (compare on and off diagonal elements in Figure 7). RSQsim does, therefore, produce synthetic earthquakes involving slip on multiple, spatially-separated faults. Fault surfaces in our models are no closer than 500 m (section 3.2). This result is not trivial, since, as discussed in section 3.1, RSQsim is a quasi-static simulator, whose treatment of earthquake rupture behaviour is effectively designed to emulate the propagation of slip in (single fault) earthquakes, rather than detailed reproduction of the physics of rupture dynamics. The occurrence of synthetic, multi-fault earthquakes implies that the approach of weakening patches within a small area around patches which are slipping is a successful method of rupture emulation (Dieterich, 1995).

5.1.1 Proportion of synthetic earthquakes which are multi-fault

The relative number of single- and multi-fault earthquakes varies widely between faults (and depends on the synthetic catalogue, section 5.3). End-member examples are Hope Hanmer NW, which only ruptures in multi-fault synthetic earthquakes, and the Palliser-Kaiwhata fault in the 'No Interface' catalogue, which only ruptures in single-fault events (although this is not

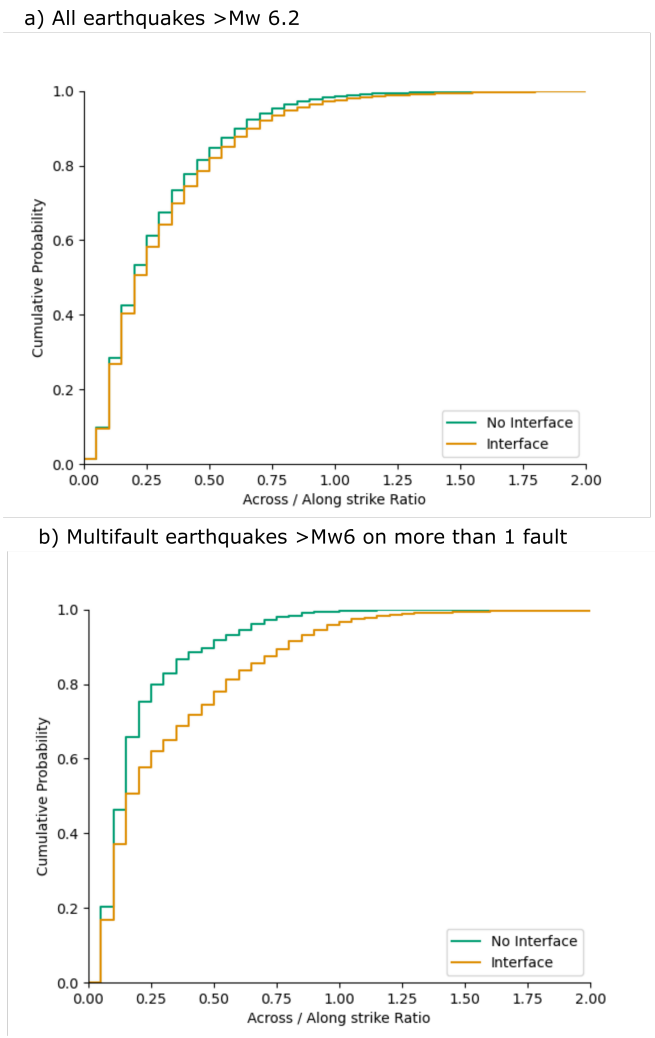

Figure 9 Cumulative histograms of the aspect ratios (ratio of strike-parallel to strike-perpendicular rupture dimension) of the upper crustal component of earthquakes in our RSQsim catalogues, i.e. neglecting the distribution of slip on the subduction interface. a) shows the aspect ratios of all earthquakes with M_w>6.2 in these catalogues (equivalent to 2 M_w 6 earthquakes), whereas b) shows the aspect ratios of multi-fault earthquakes, using the definition of at least 2 faults having a moment release equivalent to M_w 6. Orange lines show the 'Interface' catalogue, green lines show the 'No Interface' catalogue.

the case in the 'Interface' catalogue). The diversity of behaviour and proportions of single-fault and multi-fault ruptures suggests that RSQsim is able to capture some of the complexities of how different faults interact and contribute to each other's stress state, consistent with observations of e.g. the Papatea fault, which may experience its largest displacements in multi-fault earthquakes (e.g. Langridge et al., 2018; Diederichs et al., 2019) but may also rupture in single fault earthquakes (Langridge et al., 2023). We note, however, that we do not expect the homogeneous elastic medium in which faults are embedded in RSQsim to reproduce the detailed behaviour of faults, such as the Papatea fault, which are thought to show anelastic loading behaviour (Diederichs et al., 2019).

The proportion of synthetic earthquakes which involve multiple faults increases with earthquake magnitude, for both of our catalogues and for all definitions of 'multi-fault' (Figure 5). All but one of the synthetic earthquakes above M_W 8 in the 'No Interface' catalogue, and 97% of those in the 'Interface' catalogue, involve rupture on more than one fault. This increasing proportion of multi-fault synthetic earthquakes at high magnitude, is consistent with Nicol et al. (2016)'s suggestion that the individual faults involved in multi-fault ruptures in A-NZ still follow their 'characteristic' magnitude-area scaling. In this case, the area of each individual fault would determine the maximum magnitude of earthquake which it is able to host (e.g. Wells and Coppersmith, 1994; Stirling et al., 2023) such that there are limited faults with sufficient area to host earthquakes with $M_w > 8$, requiring multiple faults to be involved in the largest earthquakes (particularly in the 'No Interface' catalogue, discussed further in section 5.3). This result is also consistent with observation records of global earthquakes compiled by Quigley et al. (2017), who found that the proportion of earthquakes involving multiple faults (and the number of faults involved) increased with earthquake magnitude.

Our results also suggest, however, that it is likely that the more detailed our observations of an earthquake, the more likely it is to appear complex or multi-fault. Even the most restrictive definition of a multi-fault earthquake which we use here may not be suffi-

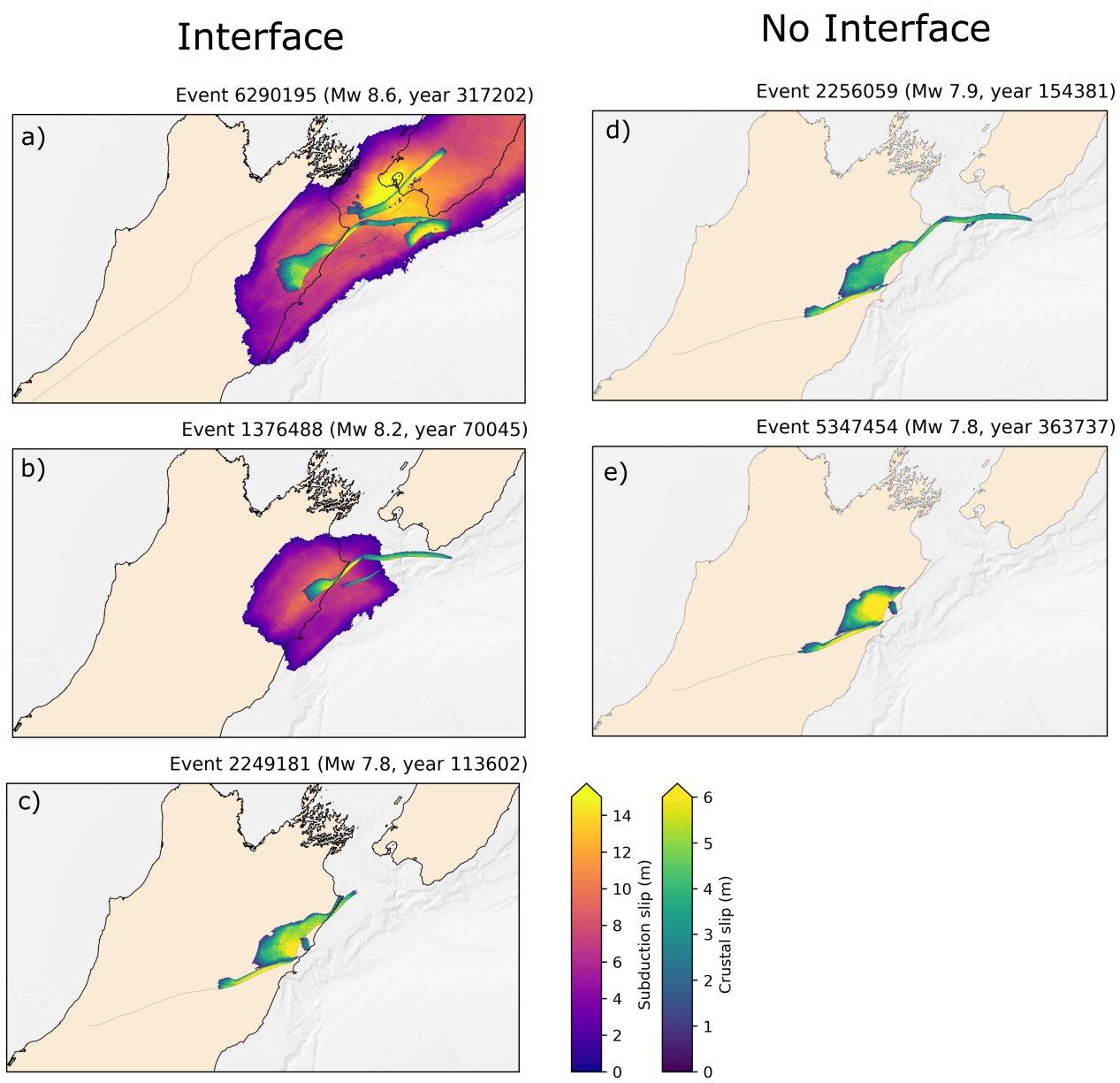

Figure 10 Examples of 'Kaikōura-like' earthquakes from the 'Interface' (a, b, c) and 'No Interface' catalogues (d, e). c) shows a rare (n=2) Kaikōura-like event in the 'Interface' catalogue which does not involve the subduction interface.

cient for an earthquake to be observable paleoseismologically, yet there is already a significant increase in the times between synthetic multi-fault earthquakes using our least and most restrictive definitions (any slip on more than one fault vs surface slip and more than one fault with an effective magnitude release $>M_w6$, Figure 5).

The definitions of "multi-fault" which we use here are appropriate – and tractable – conditions for our synthetic earthquake catalogues, where the specific faults which rupture are well defined, but are somewhat different from those used in the literature. Quigley et al. (2017), for example, require multi-fault earthquakes to rupture faults separated by less than 10 km with a pause between these ruptures of no more than 20 s. We return to the temporal gap used in section 5.1.2 below. Those authors also define fault segments as part of the same fault kinematically if the angular change in strike between contiguous segments is $<30°$. These criteria are less relevant for the simulator context where the synthetic slip on each fault is known and faults are prespecified, which raises important questions about the detectability of multi-fault involvement in earthquakes, and how to compare synthetic catalogues to observed catalogues. Importantly, although we see complex multi-fault synthetic earthquakes in our catalogues, these are still bounded i.e. we do not see any events with full rupture of all faults. These bounded multi-fault earthquakes suggest that the stress-propagation in RSQsim does limit the lateral extent of rupture, and how these limits compare to those from e.g. the plausibility filter approach used by UCERF3 (Milner et al., 2021)

and the A-NZ National Seismic Hazard Model (Gerstenberger et al., 2024b), is an important area for future research.

5.1.2 Recurrence intervals of synthetic multi-fault earthquakes

Of the definitions we use for a 'multi-fault' earthquake, the one which is most similar to expected observational bounds is surface rupture on more than one fault and more than one fault has an effective magnitude release equivalent to $>M_w$ 6 (definition 4; cf. Nicol et al., 2016; Coffey et al., 2022, although we note that 'surface rupture' in our case means at least 0.1 m of slip on a patch within 1 km of the surface, which may be an overly generous estimate for observability.) These synthetic earthquakes have a median recurrence interval of 81 and 87 years for our 'Interface' and 'No Interface' catalogues respectively (Figure 5, section 4.2.2). Nicol et al. (2022) estimated that of the eight surface-rupturing earthquakes which have been documented in A-NZ since 1840 (the initiation of written historical records), seven involved multiple faults. Their dataset gives a median interevent time of 33 years – with significant clustering – for the whole country. This median value is somewhat lower than that from the synthetic catalogue, but the discrepancy is not surprising given the small size of the observational dataset, and the larger geographic area which it spans (Nicol et al., 2022, include 3 multi-fault earthquakes outside our study area).

A key question is what causes the short times between synthetic multi-fault earthquakes in our catalogues (grey bars in figure 5). These events are closely spaced and frequently either directly along strike or involve faults closely connected in three dimensional space by the subduction interface (which may be the reason these short times between similar synthetic earthquakes are more common in the 'Interface' catalogue). These relationships suggest that these short interevent times are related to the definition of a single earthquake in RSQsim. This definition is based on shear stress, with a synthetic earthquake ending when the shear stress on all patches drops below the 'steady-state' shear stress. We specify a stress overshoot factor, such that the shear stress must drop below the steady-state shear stress minus the overshoot factor (here 0.1) multiplied by the difference between the peak shear stress in the event and the steady-state shear stress. This overshoot factor, the region over which a is reduced during the 'rupture' phase, and the amount by which a is reduced (see section 3.3), combine to control how far a synthetic earthquake propagates and when the patches move back to the 'healing' phase. As such, it is possible to have a synthetic earthquake which ruptures multiple faults, falls below the steady-state stress threshold everywhere and then exceeds that threshold again in a very short time. This situation essentially corresponds to the static stress change associated with the initial earthquake having brought the fault sufficiently close to failure that reloading is almost instantaneous. Such sequences of synthetic earthquakes are similar to earthquake doublets (e.g. Nissen et al., 2016), although we note that since RSQsim is only quasi-dynamic, such earthquakes might be more likely to be observed or considered as single events if they occurred in the real world (cf. the Kaikōura earthquake 'jumping' the Hope fault with an associated pause in moment release; Duputel and Rivera, 2017; Ulrich et al., 2019). Quigley et al. (2017), for example, use a pause in moment release of 20 s as their defining criterion for a single earthquake. The idea that some of these synthetic earthquakes would be considered as single, rather than separate, earthquakes if they were observed is consistent with the slip distributions of synthetic earthquakes with short interevent times, which tend to 'fill in' gaps in slip left by the previous multi-fault synthetic earthquake (which is often also the previous synthetic earthquake), or to continue the propagation of slip along strike.

5.1.3 Implications for comparisons between synthetic and observational earthquake catalogues

Our results demonstrate the need to be very clear both about which earthquakes our observational, historical and paleoseismic records are likely to capture (cf. Nicol et al., 2016; Coffey et al., 2022), and the modelling choices which underpin the synthetic earthquake catalogues before we can make appropriate, detailed comparisons between synthetic and observed catalogues. To ensure that tests of earthquake simulators are robust we must ensure our definitions are consistent, paying careful attention to the probability of detection using different methods, and appropriately reducing the information content of synthetic catalogues. This caveat also applies to earthquakes on single faults.

A key example of the challenge in comparing observed and synthetic earthquake records is in the definition of multi-fault earthquakes. As discussed in section 5.1.1, our results suggest a scale- and resolution-dependence to the proportion of multi-fault earthquakes. The scarcity of multi-fault earthquakes in paleoseismological records has already been suggested to be, at least in part, an issue of low resolution in earthquake timing preventing precise correlation between earthquakes rupturing different faults (Clark et al., 2015; Humphrey et al., 2025). The 2010 Darfield earthquake, which would not have been resolvably multi-fault prior to the advent of InSAR and GNSS (Beavan et al., 2012) clearly demonstrates that the complexity of an earthquake is likely a function of the scale of our observations. How to compare between inherently uncertain observations and inherently simplified models is, therefore a key challenge.

Overall, our results suggest that both seismic hazard analysis and paleoseismological interpretations need to account for the possibility of multi-fault earthquakes (e.g. Valentini, 2021; Humphrey et al., 2025) and their effects on earthquake slip budgets (e.g. Howell and Clark, 2022).

5.2 Can RSQsim produce synthetic earthquakes with similar properties to the 2016 Kaikōura earthquake?

As for 'multi-fault' earthquakes, the use of earthquake simulators renders the definition of what constitutes a 'Kaikōura-like' earthquake challenging. Here we have called synthetic earthquakes 'Kaikōura-like' if they have M_w >7.5, involve ≥ 4 faults with effective magnitude release within 1.5 magnitude units of the effective magnitude released by the principal fault and have an effective magnitude of at least M_w7 on the Jordan-Kekerengu-Needles fault. Using this operational definition, the median time between Kaikōura-like synthetic earthquakes in our 'Interface' catalogue is 2150 years, consistent with the recurrence interval proposed by Brough et al. (2023) for The Humps fault and Kaikōura-like earthquakes.

These synthetic earthquakes reproduce some of the complexity of the 2016 Kaikōura earthquake, suggesting that RSQsim may be a useful tool to generate example earthquakes beyond those which have been observed but which are consistent with physical stress transfer. Applications to potential future earthquakes are not currently a common use of dynamic earthquake simulators, which have largely focussed on investigating the conditions required to reproduced observed earthquakes (e.g. Ando and Kaneko, 2018; Ulrich et al., 2019). Such scenario earthquakes could be useful for seismic hazard and risk analysis, particularly generating realistic slip and shaking scenarios (e.g. Howell et al., 2023b).

However, the synthetic earthquakes in our catalogues also have some features which are not consistent with observations from 2016. Specifically: 1) the subduction interface (almost) always releases most of the seismic moment for our synthetic earthquakes (discussed further in section 5.3), 2) we do not see any instances of earthquakes initiating south of the Hope fault and propagating on to faults to its north and 3) the 'Kaikōura-like' events not involving the subduction interface (in both the 'Interface' and 'No Interface' catalogues, figures 10) all involve the Hope fault, which did not rupture in 2016.

These inconsistencies with specific features of the 2016 earthquake suggests a number of possibilities. First, the quasi-static rupture approximation of RSQsim may not adequately capture the dynamic stress transfer involved in the Kaikōura earthquake (e.g. Ando and Kaneko, 2018; Ulrich et al., 2019). Alternatively, simultaneous rupture of the specific combination of faults involved in the Kaikōura earthquake may simply be extremely rare (consistent with the findings of e.g. Walsh et al., 2023). The 2 kyr return times discussed by Brough et al. (2023) are specifically based on evidence for the rupture of The Humps fault, so do not have to involve the same combination of faults involved in the 2016 earthquake.

5.3 What is the role of the Hikurangi subduction interface in controlling synthetic multi-fault earthquakes?

The similarities and differences between our 'Interface' and 'No Interface' catalogues offer insights into the role of the Hikurangi subduction interface in controlling the proportion of earthquakes which are multi-fault and the recurrence interval, magnitude and geometry of such earthquakes. The first published RSQsim catalogue for A-NZ (Shaw et al., 2022) used a planar geometry for the subduction interface. The Williams et al. (2013) model we use here allows us to investigate how a more realistic subduction interface might interact with faults in the overriding Australian plate. We note, however, that, although the geometry of the interface is more realistic in our model than in previous iterations, the limitations of RSQsim and our fault modelling techniques, particularly not having listric faults and using a homogeneous elastic medium, mean that these comparisons are more indicative of the effects of having a connecting structure underlying a subset of the crustal faults than of the full complexity of a subduction interface (e.g. effects of fluids Bassett et al., 2014, and frictional heterogeneity, Boulton et al. (2019)).

The most straightforward effect of including the subduction interface in our models is increased productivity and a higher maximum magnitude (M_w8.7 as compared to M_w8.1 with no interface). Similarly, a lower proportion of large synthetic earthquakes involve multiple faults in our 'Interface', compared to our 'No Interface' catalogue because individual faults in the 'No Interface' catalogue have insufficient area to host synthetic earthquakes >∼M_w8. These findings are a first-order check on our results – the large area of the subduction interface means that we would expect it to produce large earthquakes (as observed in subduction zones globally) and having an additional large fault with a non-zero slip rate would be expected to significantly increase productivity.

Both of our catalogues contain multi-fault synthetic earthquakes (section 5.1), with similar inter-event times (Figure 5). For the 'No Interface' catalogue, these multi-fault synthetic earthquakes primarily involve along-strike, adjacent faults (Figure 7), suggesting that the proximity of upper-crustal faults plays an important role in allowing multi-fault earthquakes, such that fault network geometry is likely to be a key control on earthquake magnitude and timing (cf. Robinson, 2004; Howarth et al., 2021).

There are, however, almost no 'complex' multi-fault synthetic earthquakes in the 'No Interface' catalogue (Figure 6, where 'complex' multi-fault is defined as M_w >7.5, involving ≥4 faults with effective magnitude release within 1.5 magnitude units of the highest effective magnitude released by the principal fault, section 3.4). Those which do occur are similar to the (also limited) crustal-only complex multi-fault synthetic earthquakes in the 'Interface' catalogue (compare figures 10c and e).

This lack of 'complex' synthetic earthquakes may be related to our specific definition, i.e. there are few such synthetic earthquakes because there are relatively few faults in the 'No Interface' model capable of generating large synthetic earthquakes, unlike the 'Interface' catalogue where the subduction interface can easily increase the moment sufficiently to meet at least the magnitude criterion. The 'No Interface' catalogue also contains fewer faults which are within the stress influence of another such fault such that they can co-rupture. The

latter point highlights the key insight from our different catalogues: the subduction interface facilitates stress transfer between crustal faults.

We see this facilitation of stress transfer both in the greater complexity of multi-fault synthetic earthquakes in the 'Interface' earthquake and in the faults involved in multi-fault synthetic earthquakes in our two catalogues. Our results in section 4.2.3 show that synthetic earthquakes in the 'Interface' catalogue tend to have higher aspect ratios (be more 'square' in map view) than those in the 'No Interface' catalogue. That is, the along- and across-strike widths of synthetic earthquakes are more similar in the 'Interface' catalogue. Such ruptures would potentially be excluded by the plausibility filters used in seismic hazard analyses such as UCERF3 (Milner et al., 2022) and the New Zealand National Seismic Hazard model (Gerstenberger et al., 2022, 2024a). In contrast, synthetic earthquakes in the 'No Interface' catalogue tend to be long and narrow, likely more consistent with plausibility filters. These aspect ratios are consistent with the observation that, at least for the fastest slip rate faults, co-ruptures in the 'Interface' catalogue frequently involve faults which are sub-parallel and across strike from each other, whereas those in the 'No Interface' catalogue are typically adjacent to, and along-strike from, each other.

As discussed in sections 3.3 and 5.1.2, stress transfer during a synthetic earthquake in RSQsim depends on the proximity of fault patches (and additionally which ones are weakened during the 'rupture' phase). As a result, the proximity of the subduction interface to the base of multiple crustal faults means that it is likely to drive rupture on these faults (seen from the dominance of the Hikurangi subduction interface as the hypocentral fault of complex multi-fault synthetic earthquakes). Crucially, the proximity of faults needs to be considered in three dimensions, particularly in areas such as the Marlborough fault system with a large number of dipping faults. The proximity of fault traces is frequently not the closest distance between such faults, and proximity at depth can also facilitate stress transfer.

Lamb et al. (2018) argued that the subduction interface is the only structure required to drive stress transfer on the crustal faults of the Marlborough Fault System, whilst other authors have suggested that the deformation in this region is purely crustal (e.g. Reyners, 1998). We suggest an intermediate position where the interface provides a key linking structure driving stress transfer between crustal faults, but the geometry of the crustal faults drives details of their strain accumulation and rupture, particularly for multi-fault earthquakes and faults which are proximal at depth. Such an interpretation is consistent with Nicol et al. (2022)'s suggestion that the faults which have co-ruptured in historical multi-fault earthquakes in A-NZ are 'hard-linked' at depth, and with Page (2021)'s proposal that greater fault connectivity is needed in seismic hazard models in order to capture potential fault linkages. There is increasing evidence for such combined subduction- upper plate earthquakes, both in Aotearoa-New Zealand (Darby and Beanland, 1992; Pizer et al., 2023; Humphrey et al., 2025) and globally (Gomberg and Sherrod, 2014), and earthquake simulators may provide a viable starting point to understand their potential consequences in the absence of contemporary observations (cf. Robinson and Benites, 1996).

The discussion above focuses specifically on the Hikurangi subduction interface, but the same role could be performed by a different low-angle thrust fault underlying multiple crustal faults at relatively shallow depths. It is also worth noting that it is the large spatial extent of the subduction interface, rather than a particularly high slip rate, which facilitates this stress transfer (the slip rate is 5-10 mm yr^{-1} under much of the Kaikōura region and $<$5mm yr^{-1} further south, Figure 2). Our results therefore have little to say about precisely which low-angle thrust was involved in the 2016 Kaikōura earthquake, but suggest that any such structure is likely to have had an important influence on the complexity of that earthquake. We also suggest that the role of the subduction interface as a connecting structure makes it particularly important to understand the interface's shape and location. If there is a seismogenic subduction interface beneath the Marlborough and North Canterbury region, even with a low slip rate, our results suggest that it may facilitate large earthquakes, and earthquakes, such as the 2016 Kaikōura event (e.g. Herman et al., 2023), where crustal faults rupture with slip higher that expected from magnitude-scaling relations.

5.4 Limitations and future work

Our models represent an improvement to previous physics-based synthetic catalogues for A-NZ, and the first investigation of the potential utility of such simulations in understanding multi-fault ruptures, specifically those similar to the 2016 Kaikōura earthquake. However, these simulations have a number of limitations which would benefit from further exploration.

Two key areas for further exploration which are within the current capabilities of RSQsim are the role of fault network geometry and frictional parameters. Delogkos et al. (2023) demonstrated the importance of geometric complexity in controlling the outputs of RSQsim. There are significant debates about the geometry of the fault network in the North Canterbury and Marlborough region (e.g. see comments in the NZCFM; Seebeck et al., 2022, 2023), which suggest that it would be illuminating to run further simulations with a range of plausible geometries in order to investigate their impacts on synthetic earthquakes. Liao et al. (2024) have demonstrated the importance of frictional parameters, and particularly frictional heterogeneity in RSQsim catalogues. The frictional properties of faults in the Marlborough region are generally poorly constrained, which motivated our use of uniform frictional properties in this model. The frictional properties of these faults are likely to be heterogeneous (e.g. Boulton et al., 2018; Eberhart-Phillips et al., 2021; Brideau et al., 2022), so future work should explore the effects of heterogeneity as well as the appropriate conversions between conventional rate and state friction parameters and the simplified parameters used in RSQsim.

We have used RSQsim to explore the effects of the subduction interface (or a similar, low-angle structure, section 5.3) on synthetic earthquakes in central Aotearoa-New Zealand. As discussed in section 2, there is still debate as to whether the subduction interface – in the sense of an active megathrust accommodating at least some of the plate convergence rate – extends as far south as in our model (Upton et al., 2025). Understanding the location of active deformation in North Canterbury and how strain is transferred to the Alpine Fault, is crucial for a more complete understanding of seismic hazard across the northern South Island. The choice to include a laterally-extensive subduction interface is one of many made in conducting this modelling, which express our assumptions and current understanding. It is important to remember, and continue to distinguish synthetic earthquakes from those which have actually been observed, particularly where our results (e.g. section 5.1.3) suggest that direct comparisons are not trivial and require significant further work.

There is a more general challenge that using physics-based simulators to extend the range of potential future earthquakes beyond the constraints of the historical record comes with a loss of observational constraints on the plausibility of earthquakes. How to ensure that synthetic catalogues are consistent with observational evidence whilst remaining unconstrained by the limited imaginations of scientists, is perhaps the greatest challenge to the future use of such simulators and requires critical reflection in addition to the development and application of rigorous statistical methodologies, which account for the limitations of both observational data and synthetic catalogues.

6 Conclusions

We have made two 450 kyr synthetic earthquake catalogues for central A-NZ using a physics-based earthquake simulator. These catalogues are both a tool for investigating earthquakes in this region, and a demonstration of a new methodology for constructing models of 3D fault networks (Howell et al., in review). We are able to reproduce the scaling relations observed in the study area. Our catalogues contain numerous multi-fault earthquakes, allowing us to investigate the properties and temporal relationships of such events. The Hikurangi subduction interface appears to play a key role in allowing stress transfer between faults in our models, particularly for complex multi-fault earthquakes, or those similar to the 2016 Kaikōura earthquake. We find that the times between 'Kaikōura -like' events in our model are consistent with proposed return times from paleoseismology, but that we are unable to reproduce the specific features of the 2016 earthquake. These findings suggest that:

1. There is significant potential for multi-fault, multi-cycle earthquake simulators to extend the range of earthquakes considered in seismic hazard analyses beyond those observed in the historical record.
2. Such simulations can produce complex multi-fault earthquakes.
3. The Kaikōura earthquake in 2016 was likely dominated by dynamic stress transfer, by interactions between faults with geometries different from those used in this study or represented an extremely rare event.

Acknowledgements

This work was initiated through Resilience to Nature's Challenges 2 National Science Challenge funding to CP, AH, AN & BF. CP, AH & AN received funding from the Ministry of Business, Innovation & Employment Endeavour-funded project, Ngā Ngaru Wakapuke. The authors wish to acknowledge the use of New Zealand eScience Infrastructure (NeSI) high performance computing facilities and consulting support as part of this research. New Zealand's national facilities are provided by NeSI and funded jointly by NeSI's collaborator institutions and through the Ministry of Business, Innovation & Employment's Research Infrastructure programme. URL https://www.nesi.org.nz. Some figures were created using the Generic Mapping Tools (Wessel et al., 2019).

Data and code availability

Kaikōura earthquake surface ruptures can be downloaded from https://data.gns.cri.nz/af/ (last accessed 4/12/25). The fault combination and hierarchy folders, map inputs, final fault meshes, RSQsim input and output files and scripts for figure creation and data analysis can be found on Zenodo: https://doi.org/10.5281/zenodo.17862180.

Competing interests

The authors have no competing interests.

7 References

References

Abdrakhmatov, K. E., Walker, R. T., Campbell, G. E., Carr, A. S., Elliott, A., Hillemann, C., Hollingsworth, J., Landgraf, A., Mackenzie, D., Mukambayev, A., Rizza, M., and Sloan, R. A. Multisegment Rupture in the 11 July 1889 Chilik Earthquake (Mw 8.0–8.3), Kazakh Tien Shan, Interpreted from Remote Sensing, Field Survey, and Paleoseismic Trenching. *Journal of Geophysical Research : Solid Earth*, 121:4615–4640, 2016. doi: 10.1002/2012JB010016.1.

Anderson, H., Webb, T., and Jackson, J. Focal Mechanisms of Large Earthquakes in the South Island of New Zealand: Implications for the Accommodation of Pacific-Australia Plate Motion. *Geophysical Journal International*, 115(3):1032–1054, Dec. 1993. doi: 10.1111/j.1365-246X.1993.tb01508.x.

Anderson, J. G., Biasi, G. P., Angster, S., and Wesnousky, S. G. Improved Scaling Relationships for Seismic Moment and Average Slip of Strike-Slip Earthquakes Incorporating Fault-Slip Rate, Fault Width, and Stress Drop. *Bulletin of the Seismological Society of America*, 111(5):2379–2392, Oct. 2021. doi: 10.1785/0120210113.

Ando, R. Fast Domain Partitioning Method for Dynamic Boundary Integral Equations Applicable to Non-Planar Faults Dipping in 3-D Elastic Half-Space. *Geophysical Journal International*, 207(2): 833–847, Nov. 2016. doi: 10.1093/gji/ggw299.

Ando, R. and Kaneko, Y. Dynamic Rupture Simulation Reproduces Spontaneous Multifault Rupture and Arrest during the 2016 Mw 7.9 Kaikoura Earthquake. *Geophysical Research Letters*, 45(23): 12,875–12,883, Dec. 2018. doi: 10.1029/2018GL080550.

Bai, Y., Lay, T., Cheung, K. F., and Ye, L. Two Regions of Seafloor Deformation Generated the Tsunami for the 13 November 2016, Kaikoura, New Zealand Earthquake. *Geophysical Research Letters*, 44(13):6597–6606, July 2017. doi: 10.1002/2017gl073717.

Barnes, P. M. Continental Extension of the Pacific Plate at the Southern Termination of the Hikurangi Subduction Zone: The North Mernoo Fault Zone, Offshore New Zealand. *Tectonics*, 13 (4):735–754, Aug. 1994. doi: 10.1029/94TC00798.

Barnes, P. M. and Audru, J.-C. Quaternary Faulting in the Offshore Flaxbourne and Wairarapa Basins, Southern Cook Strait, New Zealand. *New Zealand Journal of Geology and Geophysics*, 42(3): 349–367, Sept. 1999a. doi: 10.1080/00288306.1999.9514851.

Barnes, P. M. and Audru, J.-C. Recognition of Active Strike-Slip Faulting from High-Resolution Marine Seismic Reflection Profiles: Eastern Marlborough Fault System, New Zealand. *Geological Society of America Bulletin*, 111(4):538–559, Apr. 1999b. doi: 10.1130/0016-7606(1999)111<0538:roassf>2.3.co;2.

Barnes, P. M. and De Lépinay, B. M. Rates and Mechanics of Rapid Frontal Accretion along the Very Obliquely Convergent Southern Hikurangi Margin, New Zealand. *Journal of Geophysical Research: Solid Earth*, 102(B11):24931–24952, Nov. 1997. doi: 10.1029/97JB01384.

Barnes, P. M., Nicol, A., and Harrison, T. Late Cenozoic Evolution and Earthquake Potential of an Active Listric Thrust Complex above the Hikurangi Subduction Zone, New Zealand. *Geological Society of America Bulletin*, 114(11):1379–1405, Nov. 2002. doi: 10.1130/0016-7606(2002)114<1379:LCEAEP>2.0.CO;2.

Barrell, D. and Townsend, D. General Distribution and Characteristics of Active Faults and Folds in the Hurunui District, North Canterbury. GNS Science Consultancy Report 2012/113, GNS Science, 2012.

Bassett, D., Sutherland, R., and Henrys, S. Slow Wavespeeds and Fluid Overpressure in a Region of Shallow Geodetic Locking and Slow Slip, Hikurangi Subduction Margin, New Zealand. *Earth and Planetary Science Letters*, 389:1–13, Mar. 2014. doi: 10.1016/j.epsl.2013.12.021.

Beavan, J., Samsonov, S., Motagh, M., Wallace, L., Ellis, S., and Palmer, N. The Darfield (Canterbury) Earthquake. *Bulletin of the New Zealand Society for Earthquake Engineering*, 43(4):228–235, Dec. 2010. doi: 10.5459/bnzsee.43.4.228-235.

Beavan, J., Motagh, M., Fielding, E. J., Donnelly, N., and Collett, D. Fault Slip Models of the 2010–2011 Canterbury, New Zealand, Earthquakes from Geodetic Data and Observations of Postseismic Ground Deformation. *New Zealand Journal of Geology and Geophysics*, 55(3):207–221, Sept. 2012. doi: 10.1080/00288306.2012.697472.

Berryman, K. R., Cochran, U. A., Clark, K. J., Biasi, G. P., Langridge, R. M., and Villamor, P. Major Earthquakes Occur Regularly on an Isolated Plate Boundary Fault. *Science*, 336(6089):1690–1693, June 2012. doi: 10.1126/science.1218959.

Boulton, C., Barth, N. C., Moore, D. E., Lockner, D. A., Townend, J., and Faulkner, D. R. Frictional Properties and 3-D Stress Analysis of the Southern Alpine Fault, New Zealand. *Journal of Structural Geology*, 114:43–54, Sept. 2018. doi: 10.1016/j.jsg.2018.06.003.

Boulton, C., Niemeijer, A. R., Hollis, C. J., Townend, J., Raven, M. D., Kulhanek, D. K., and Shepherd, C. L. Temperature-Dependent Frictional Properties of Heterogeneous Hikurangi Subduction Zone Input Sediments, ODP Site 1124. *Tectonophysics*, 757:123–139, Apr. 2019. doi: 10.1016/j.tecto.2019.02.006.

Brideau, M.-A., Massey, C. I., Carey, J. M., and Lyndsell, B. Geomechanical Characterisation of Discontinuous Greywacke from the Wellington Region Based on Laboratory Testing. *New Zealand Journal of Geology and Geophysics*, 65(2):265–282, Apr. 2022. doi: 10.1080/00288306.2020.1853181.

Brough, T., Nicol, A., Stahl, T., Pettinga, J. R., Van Dissen, R., Clark, D., Khajavi, N., Pedley, K., Langridge, R., and Wang, N. Paleoseismicity of the Western Humps Fault on the Emu Plain, North Canterbury, New Zealand. *New Zealand Journal of Geology and Geophysics*, 66(2):279–292, Apr. 2023. doi: 10.1080/00288306.2021.1986727.

Cesca, S., Zhang, Y., Mouslopoulou, V., Wang, R., Saul, J., Savage, M., Heimann, S., Kufner, S. K., Oncken, O., and Dahm, T. Complex Rupture Process of the Mw 7.8, 2016, Kaikoura Earthquake, New Zealand, and Its Aftershock Sequence. *Earth and Planetary Science Letters*, 478:110–120, 2017. doi: 10.1016/j.epsl.2017.08.024.

Chamberlain, C. J., Frank, W. B., Lanza, F., Townend, J., and Warren-Smith, E. Illuminating the Pre-, Co-, and Post-Seismic Phases of the 2016 M7.8 Kaikōura Earthquake With 10 Years of Seismicity. *Journal of Geophysical Research: Solid Earth*, 126(8): e2021JB022304, Aug. 2021. doi: 10.1029/2021JB022304.

Clark, K., Nissen, E. K., Howarth, J. D., Hamling, I. J., Mountjoy, J. J., Ries, W. F., Jones, K., Goldstien, S., Cochran, U. A., Villamor, P., Hreinsdóttir, S., Litchfield, N. J., Mueller, C., Berryman, K. R., and Strong, D. T. Highly Variable Coastal Deformation in the 2016 M W 7.8 Kaikōura Earthquake Reflects Rupture Complexity along a Transpressional Plate Boundary. *Earth and Planetary Science Letters*, 474:334–344, 2017. doi: 10.1016/j.epsl.2017.06.048.

Clark, K., Howarth, J., Litchfield, N., Cochran, U., Turnbull, J., Dowling, L., Howell, A., Berryman, K., and Wolfe, F. Geological Evidence for Past Large Earthquakes and Tsunamis along the Hikurangi Subduction Margin, New Zealand. *Marine Geology*, 412: 139–172, June 2019. doi: 10.1016/J.MARGEO.2019.03.004.

Clark, K. J., Hayward, B. W., Cochran, U. A., Wallace, L. M., Power, W. L., and Sabaa, A. T. Evidence for Past Subduction Earthquakes at a Plate Boundary with Widespread Upper Plate Faulting: Southern Hikurangi Margin, New Zealand. *Bulletin of the*

Seismological Society of America, 105(3):1661–1690, June 2015. doi: 10.1785/0120140291.

Coffey, G., Rollins, C., Dissen, R. V., Rhoades, D., Thingbaijam, K., Clark, K., Gerstenberger, M., Litchfield, N., and Nicol, A. New Zealand National Seismic Hazard Model 2022: Earthquake Recurrence Derivation from Paleoseismic Data and Probability of Surface Fault Rupture Detection, 2022. doi: 10.21420/2YWK-ZE30.

Coffey, G., Langridge, R. M., Litchfield, N. J., Van Dissen, R. J., and Clark, K. J. Paleoearthquakes at the Junction of the Tokomaru and Northern Ōhāriu Faults, Implications for Fault Interactions in the Southern North Island, New Zealand. *New Zealand Journal of Geology and Geophysics*, pages 1–15, Oct. 2023. doi: 10.1080/00288306.2023.2263403.

Darby, D. J. and Beanland, S. Possible Source Models for the 1855 Wairarapa Earthquake, New Zealand. *Journal of Geophysical Research: Solid Earth*, 97(B9):12375–12389, Aug. 1992. doi: 10.1029/92jb00567.

Delogkos, E., Howell, A., Seebeck, H., Shaw, B. E., Nicol, A., Mika Liao, Y.-W., and Walsh, J. J. Impact of Variable Fault Geometries and Slip Rates on Earthquake Catalogs From Physics-Based Simulations of a Normal Fault. *Journal of Geophysical Research: Solid Earth*, 128(11):e2023JB026746, Nov. 2023. doi: 10.1029/2023JB026746.

DeMets, C., Gordon, R. G., and Argus, D. F. Geologically Current Plate Motions. *Geophysical Journal International*, 181(1):1–80, Apr. 2010. doi: 10.1111/j.1365-246X.2009.04491.x.

Diederichs, A., Nissen, E. K., Lajoie, L. J., Langridge, R. M., Malireddi, S. R., Clark, K. J., Hamling, I. J., and Tagliasacchi, A. Unusual Kinematics of the Papatea Fault (2016 Kaikōura Earthquake) Suggest Anelastic Rupture. *Science Advances*, 5(10): eaax5703, Oct. 2019. doi: 10.1126/sciadv.aax5703.

Dieterich, J. H. Earthquake Simulations with Time-Dependent Nucleation and Long-Range Interactions. *Nonlinear Processes in Geophysics*, 2(3/4):109–120, Dec. 1995. doi: 10.5194/npg-2-109-1995.

Dieterich, J. H. and Richards-Dinger, K. B. Earthquake Recurrence in Simulated Fault Systems. In Savage, M. K., Rhoades, D. A., Smith, E. G. C., Gerstenberger, M. C., and Vere-Jones, D., editors, *Seismogenesis and Earthquake Forecasting: The Frank Evison Volume II*, pages 233–250. Springer Basel, Basel, 2010. doi: 10.1007/978-3-0346-0500-7$_1$5.

Downes, G. L. Procedures and Toolsused in the Investigationof New Zealand's Historical Earthquakes. *Annals of Geophysics*, 47 (2-3), Dec. 2004. doi: 10.4401/ag-3309.

Duputel, Z. and Rivera, L. Long-Period Analysis of the 2016 Kaikoura Earthquake. *Physics of the Earth and Planetary Interiors*, 265:62–66, Apr. 2017. doi: 10.1016/j.pepi.2017.02.004.

Eberhart-Phillips, D. and Reyners, M. Continental Subduction and Three-Dimensional Crustal Structure: The Northern South Island, New Zealand. *Journal of Geophysical Research: Solid Earth*, 102(B6):11843–11861, June 1997. doi: 10.1029/96JB03555.

Eberhart-Phillips, D., Reyners, M., Bannister, S., Chadwick, M., and Ellis, S. Establishing a Versatile 3-D Seismic Velocity Model for New Zealand. *Seismological Research Letters*, 81(6):992–1000, Nov. 2010. doi: 10.1785/gssrl.81.6.992.

Eberhart-Phillips, D., Ellis, S., Lanza, F., and Bannister, S. Heterogeneous Material Properties—as Inferred from Seismic Attenuation—Influenced Multiple Fault Rupture and Ductile Creep of the Kaikoura *M* w 7.8 Earthquake, New Zealand. *Geophysical Journal International*, 227(2):1204–1227, Aug. 2021. doi: 10.1093/gji/ggab272.

Ellis, S. M., Bannister, S., Van Dissen, R. J., Eberhart-Phillips, D., Holden, C., Boulton, C., Reyners, M. E., Funnell, R. H., Mortimer, N., and Upton, P. New Zealand Fault-Rupture Depth Model v1.0: A Provisional Estimate of the Maximum Depth of Seismic Rupture on New Zealand's Active Faults. *GNS science report*, 2021. doi: 10.21420/4Q75-HZ73.

Faulkner, D., Jackson, C., Lunn, R., Schlische, R., Shipton, Z., Wibberley, C., and Withjack, M. A Review of Recent Developments Concerning the Structure, Mechanics and Fluid Flow Properties of Fault Zones. *Journal of Structural Geology*, 32(11):1557–1575, Nov. 2010. doi: 10.1016/j.jsg.2010.06.009.

Field, E. H. How Physics-Based Earthquake Simulators Might Help Improve Earthquake Forecasts. *Seismological Research Letters*, 90(2A):467–472, Mar. 2019. doi: 10.1785/0220180299.

Field, E. H., Jordan, T. H., Page, M. T., Milner, K. R., Shaw, B. E., Dawson, T. E., Biasi, G. P., Parsons, T., Hardebeck, J. L., Michael, A. J., Weldon, R. J., Powers, P. M., Johnson, K. M., Zeng, Y., Felzer, K. R., Elst, N. V. D., Madden, C., Arrowsmith, R., Werner, M. J., and Thatcher, W. R. A Synoptic View of the Third Uniform California Earthquake Rupture Forecast (UCERF3). *Seismological Research Letters*, 88(5):1259–1267, Sept. 2017. doi: 10.1785/0220170045.

Fletcher, J. M., Teran, O. J., Rockwell, T. K., Oskin, M. E., Hudnut, K. W., Mueller, K. J., Spelz, R. M., Akciz, S. O., Masana, E., Faneros, G., Fielding, E. J., Leprince, S., Morelan, A. E., Stock, J., Lynch, D. K., Elliott, A. J., Gold, P., Liu-Zeng, J., González-Ortega, A., Hinojosa-Corona, A., and González-García, J. Assembly of a Large Earthquake from a Complex Fault System: Surface Rupture Kinematics of the 4 April 2010 El Mayor–Cucapah (Mexico) Mw 7.2 Earthquake. *Geosphere*, 10(4):797–827, Aug. 2014. doi: 10.1130/GES00933.1.

Gerstenberger, M. C., Bora, S. S., Bradley, B. A., DiCaprio, C., Van Dissen, R. J., Atkinson, G. M., Chamberlain, C., Christophersen, A., Clark, K. J., and Coffey, G. L. New Zealand National Seismic Hazard Model 2022 Revision : Model, Hazard and Process Overview. *GNS science report*, 2022. doi: 10.21420/TB83-7X19.

Gerstenberger, M. C., Bora, S., Bradley, B. A., DiCaprio, C., Kaiser, A., Manea, E. F., Nicol, A., Rollins, C., Stirling, M. W., Thingbaijam, K. K. S., Van Dissen, R. J., Abbott, E. R., Atkinson, G. M., Chamberlain, C., Christophersen, A., Clark, K., Coffey, G. L., De La Torre, C. A., Ellis, S. M., Fraser, J., Graham, K., Griffin, J., Hamling, I. J., Hill, M. P., Howell, A., Hulsey, A., Hutchinson, J., Iturrieta, P., Johnson, K. M., Jurgens, V. O., Kirkman, R., Langridge, R. M., Lee, R. L., Litchfield, N. J., Maurer, J., Milner, K. R., Rastin, S., Rattenbury, M. S., Rhoades, D. A., Ristau, J., Schorlemmer, D., Seebeck, H., Shaw, B. E., Stafford, P. J., Stolte, A. C., Townend, J., Villamor, P., Wallace, L. M., Weatherill, G., Williams, C. A., and Wotherspoon, L. M. The 2022 Aotearoa New Zealand National Seismic Hazard Model: Process, Overview, and Results. *Bulletin of the Seismological Society of America*, 114(1):7–36, Feb. 2024a. doi: 10.1785/0120230182.

Gerstenberger, M. C., Van Dissen, R., Rollins, C., DiCaprio, C., Thingbaijim, K. K. S., Bora, S., Chamberlain, C., Christophersen, A., Coffey, G. L., Ellis, S. M., Iturrieta, P., Johnson, K. M., Litchfield, N. J., Nicol, A., Milner, K. R., Rastin, S. J., Rhoades, D., Seebeck, H., Shaw, B. E., Stirling, M. W., Wallace, L., Allen, T. I., Bradley, B. A., Charlton, D., Clark, K. J., Fraser, J., Griffin, J., Hamling, I. J., Howell, A., Hudson-Doyle, E., Hulsey, A., Jurgens, V. O., Kaiser, A. E., Kirkman, R., Langridge, R. M., Maurer, J., Rattenbury, M. S., Ristau, J., Schorlemmer, D., Townend, J., Villamor, P., and Williams, C. The Seismicity Rate Model for the 2022 Aotearoa New Zealand National Seismic Hazard Model. *Bulletin of the Seismological Society of America*, 114(1):182–216, Feb. 2024b. doi: 10.1785/0120230165.

Gomberg, J. and Sherrod, B. Crustal Earthquake Triggering by Modern Great Earthquakes on Subduction Zone Thrusts. *Jour-*

nal of Geophysical Research: Solid Earth, 119(2):1235–1250, Feb. 2014. doi: 10.1002/2012JB009826.

Grapes, R. and Holdgate, G. Earthquake Clustering and Possible Fault Interactions across Cook Strait, New Zealand, during the 1848 and 1855 Earthquakes. *New Zealand Journal of Geology and Geophysics*, 57(3):312–330, July 2014. doi: 10.1080/00288306.2014.907579.

Hamling, I. J., Hreinsdóttir, S., Clark, K., Elliott, J., Liang, C., Fielding, E., Litchfield, N., Villamor, P., Wallace, L., Wright, T. J., D'Anastasio, E., Bannister, S., Burbidge, D., Denys, P., Gentle, P., Howarth, J., Mueller, C., Palmer, N., Pearson, C., Power, W., Barnes, P., Barrell, D. J. A., Van Dissen, R., Langridge, R., Little, T., Nicol, A., Pettinga, J., Rowland, J., and Stirling, M. Complex Multifault Rupture during the 2016 M_w 7.8 Kaikōura Earthquake, New Zealand. *Science*, 356(6334):eaam7194, Apr. 2017. doi: 10.1126/science.aam7194.

Hamling, I. J., Wright, T. J., Hreinsdóttir, S., and Wallace, L. M. A Snapshot of New Zealand's Dynamic Deformation Field From Envisat InSAR and GNSS Observations Between 2003 and 2011. *Geophysical Research Letters*, 49(2):e2021GL096465, Jan. 2022. doi: 10.1029/2021GL096465.

Hanks, T. C. A Bilinear Source-Scaling Model for M-log A Observations of Continental Earthquakes. *Bulletin of the Seismological Society of America*, 92(5):1841–1846, June 2002. doi: 10.1785/0120010148.

Hanks, T. C. and Kanamori, H. A Moment Magnitude Scale. *Journal of Geophysical Research: Solid Earth*, 84(B5):2348–2350, May 1979. doi: 10.1029/JB084iB05p02348.

Hatem, A. E., Dolan, J. F., Zinke, R. W., Van Dissen, R. J., McGuire, C. M., and Rhodes, E. J. A 2000 Yr Paleoearthquake Record along the Conway Segment of the Hope Fault: Implications for Patterns of Earthquake Occurrence in Northern South Island and Southern North Island, New Zealand. *Bulletin of the Seismological Society of America*, 109(6):2216–2239, Dec. 2019. doi: 10.1785/0120180313.

Heinecke, A., Breuer, A., Rettenberger, S., Bader, M., Gabriel, A. A., Pelties, C., Bode, A., Barth, W., Liao, X. K., Vaidyanathan, K., Smelyanskiy, M., and Dubey, P. Petascale High Order Dynamic Rupture Earthquake Simulations on Heterogeneous Supercomputers. *International Conference for High Performance Computing, Networking, Storage and Analysis, SC*, 2015-January (January):3–14, Jan. 2014. doi: 10.1109/SC.2014.6.

Herman, M. W., Furlong, K. P., and Benz, H. M. Substantial Upper Plate Faulting Above a Shallow Subduction Megathrust Earthquake: Mechanics and Implications of the Surface Faulting During the 2016 Kaikoura, New Zealand, Earthquake. *Tectonics*, 42 (5), May 2023. doi: 10.1029/2022tc007645.

Herrero-Barbero, P., Álvarez-Gómez, J. A., Williams, C., Villamor, P., Insua-Arévalo, J. M., Alonso-Henar, J., and Martínez-Díaz, J. J. Physics-Based Earthquake Simulations in Slow-Moving Faults: A Case Study from the Eastern Betic Shear Zone (SE Iberian Peninsula). *Journal of Geophysical Research: Solid Earth*, 126 (5):e2020JB021133, May 2021. doi: 10.1029/2020JB021133.

Hollingsworth, J., Ye, L., and Avouac, J. P. Dynamically Triggered Slip on a Splay Fault in the Mw 7.8, 2016 Kaikoura (New Zealand) Earthquake. *Geophysical Research Letters*, 44(8):3517–3525, Apr. 2017. doi: 10.1002/2016GL072228.

Howarth, J. D., Barth, N. C., Fitzsimons, S. J., Richards-Dinger, K., Clark, K. J., Biasi, G. P., Cochran, U. A., Langridge, R. M., Berryman, K. R., and Sutherland, R. Spatiotemporal Clustering of Great Earthquakes on a Transform Fault Controlled by Geometry. *Nature Geoscience 2021 14:5*, 14(5):314–320, Apr. 2021. doi: 10.1038/s41561-021-00721-4.

Howell, A. and Clark, K. J. Late Holocene Coseismic Uplift of the Kaikōura Coast, New Zealand. *Geosphere*, 18(3):1104–1137, June 2022. doi: 10.1130/GES02479.1.

Howell, A., Nissen, E., Stahl, T., Clark, K., Kearse, J., Van Dissen, R., Villamor, P., Langridge, R., and Jones, K. Three-Dimensional Surface Displacements During the 2016 M_W 7.8 Kaikōura Earthquake (New Zealand) From Photogrammetry-Derived Point Clouds. *Journal of Geophysical Research: Solid Earth*, 125(1): e2019JB018739, Jan. 2020. doi: 10.1029/2019JB018739.

Howell, A., Nicol, A., Bora, S., Gerstenberger, M., Van Dissen, R., Chamberlain, C., Dicaprio, C. J., Rollins, C., Stirling, M., Jurgens, O., Shaw, B. E., Howell, A., Nicol, A., Bora, S., Gerstenberger, M., Dissen, R. V., Chamberlain, C., Dicaprio, C. J., Rollins, C., Stirling, M., and Jurgens, O. Comparison of Ground-Shaking Hazard for Segmented versus Multifault Earthquake-Rupture Models in Aotearoa New Zealand. *Seismological Research Letters*, Nov. 2023a. doi: 10.1785/0220230240.

Howell, A., Penney, C., Kaiser, AE., and Fry, B. Modelling Ground Motions in the Greater Wellington Region from Multi-Fault Earthquakes in Central Aotearoa New Zealand. *GNS Science Report*, 2023b. doi: 10.21420/Z9SM-0G27.

Howell, A., McLennan, T., Penney, C., Nicol, A., Seebeck, H., Williams, C., and Fry, B. A Semi-Automated Method for Constructing Three-Dimensional Models of Complex Fault Networks. *Seismica*, in review. doi: 10.31223/X5Q422.

Hughes, L., Power, W., Lane, E. M., Savage, M. K., Arnold, R., Howell, A., Shaw, B., Fry, B., and Nicol, A. A Novel Method to Determine Probabilistic Tsunami Hazard Using a Physics-Based Synthetic Earthquake Catalog: A New Zealand Case Study. *Journal of Geophysical Research: Solid Earth*, 128(12):e2023JB027207, Dec. 2023. doi: 10.1029/2023JB027207.

Hughes, L., Lane, E. M., Power, W., Savage, M. K., Arnold, R., Howell, A., Liao, Y.-W. M., Williams, C., Shaw, B., Fry, B., and Nicol, A. Effects of Subduction Interface Locking Distributions on Tsunami Hazard: A Case Study on the Hikurangi/Tonga-Kermadec Subduction Zones. *Geophysical Journal International*, 240(2):1147–1167, Dec. 2024. doi: 10.1093/gji/ggae441.

Humphrey, J., Nicol, A., Howell, A., Litchfield, N., Langridge, R., Van Dissen, R., Penney, C., and Fry, B. Spatial and Temporal Clustering of Large Earthquakes on Upper-Plate and Subduction Thrust Faults Along the Southern Hikurangi Subduction Margin, Aotearoa-New Zealand. *Bulletin of the Seismological Society of America*, Apr. 2025. doi: 10.1785/0120240246.

Iturrieta, P., Gerstenberger, M. C., Rollins, C., Van Dissen, R., Wang, T., and Schorlemmer, D. Accounting for the Variability of Earthquake Rates within Low-Seismicity Regions: Application to the 2022 Aotearoa New Zealand National Seismic Hazard Model. *Bulletin of the Seismological Society of America*, 114(1):217–243, Feb. 2024. doi: 10.1785/0120230164.

Kaneko, Y., Ampuero, J.-P., and Lapusta, N. Spectral-Element Simulations of Long-Term Fault Slip: Effect of Low-Rigidity Layers on Earthquake-Cycle Dynamics. *Journal of Geophysical Research*, 116:10313, 2011. doi: 10.1029/2011JB008395.

Kearse, J., Little, T. A., Van Dissen, R. J., Barnes, P. M., Langridge, R., Mountjoy, J., Ries, W., Villamor, P., Clark, K. J., Benson, A., Lamarche, G., Hill, M., and Hemphill-Haley, M. Onshore to Offshore Ground-Surface and Seabed Rupture of the Jordan–Kekerengu–Needles Fault Network during the 2016 Mw 7.8 Kaikōura Earthquake, New Zealand. *Bulletin of the Seismological Society of America*, 108(3B):1573–1595, July 2018. doi: 10.1785/0120170304.

Lamb, S., Arnold, R., and Moore, J. D. Locking on a Megathrust as a Cause of Distributed Faulting and Fault-Jumping Earthquakes. *Nature Geoscience 2018 11:11*, 11(11):871–875, Oct. 2018. doi: 10.1038/s41561-018-0230-5.

Langridge, R. M., Rowland, J., Villamor, P., Mountjoy, J., Townsend, D. B., Nissen, E., Madugo, C., Ries, W. F., Gasston, C., Canva, A., Hatem, A. E., and Hamling, I. Coseismic Rupture and Preliminary Slip Estimates for the Papatea Fault and Its Role in the 2016 Mw 7.8 Kaikōura, New Zealand, Earthquake. *Bulletin of the Seismological Society of America*, 108(3B):1596–1622, July 2018. doi: 10.1785/0120170336.

Langridge, R. M., Clark, K. J., Almond, P., Baize, S., Howell, A., Kearse, J., Morgenstern, R., Deuss, K., Nissen, E., García-Mayordomo, J., and Amos, C. Late Holocene Earthquakes on the Papatea Fault and Its Role in Past Earthquake Cycles, Marlborough, New Zealand. *New Zealand Journal of Geology and Geophysics*, 66(2):317–341, Apr. 2023. doi: 10.1080/00288306.2022.2117829.

Lapusta, N., Rice, J. R., Ben-Zion, Y., and Zheng, G. Elastodynamic Analysis for Slow Tectonic Loading with Spontaneous Rupture Episodes on Faults with Rate- and State-Dependent Friction. *Journal of Geophysical Research: Solid Earth*, 105(B10):23765–23789, Oct. 2000. doi: 10.1029/2000JB900250.

Liao, Y.-W. M., Fry, B., Howell, A., Williams, C. A., Nicol, A., and Rollins, C. The Role of Heterogeneous Stress in Earthquake Cycle Models of the Hikurangi–Kermadec Subduction Zone. *Geophysical Journal International*, 239(1):574–590, Aug. 2024. doi: 10.1093/gji/ggae266.

Litchfield, N. J., Villamor, P., Dissen, R. J. V., Nicol, A., Barnes, P. M., Barrell, D. J. A., Pettinga, J. R., Langridge, R. M., Little, T. A., Mountjoy, J. J., Ries, W. F., Rowland, J., Fenton, C., Stirling, M. W., Kearse, J., Berryman, K. R., Cochran, U. A., Clark, K. J., Hemphill-Haley, M., Khajavi, N., Jones, K. E., Archibald, G., Upton, P., Asher, C., Benson, A., Cox, S. C., Gasston, C., Hale, D., Hall, B., Hatem, A. E., Heron, D. W., Howarth, J., Kane, T. J., Lamarche, G., Lawson, S., Lukovic, B., McColl, S. T., Madugo, C., Manousakis, J., Noble, D., Pedley, K., Sauer, K., Stahl, T., Strong, D. T., Townsend, D. B., Toy, V., Williams, J., Woelz, S., and Zinke, R. Surface Rupture of Multiple Crustal Faults in the 2016 Mw 7.8 Kaikōura, New Zealand, Earthquake. *Bulletin of the Seismological Society of America*, 108(3B):1496–1520, July 2018. doi: 10.1785/0120170300.

Little, T. A. and Jones, A. Seven Million Years of Strike-slip and Related Off-fault Deformation, Northeastern Marlborough Fault System, South Island, New Zealand. *Tectonics*, 17(2):285–302, Apr. 1998. doi: 10.1029/97TC03148.

Little, T. A., Van Dissen, R., Kearse, J., Norton, K., Benson, A., and Wang, N. Kekerengu Fault, New Zealand: Timing and Size of Late Holocene Surface Ruptures. *Bulletin of the Seismological Society of America*, 108(3B):1556–1572, July 2018. doi: 10.1785/0120170152.

Milner, K. R., Page, M. T., Field, E. H., Parsons, T., Biasi, G. P., and Shaw, B. E. Appendix T-defining the Inversion Rupture Set Using Plausibility Filters, 2013.

Milner, K. R., Shaw, B. E., Goulet, C. A., Richards-Dinger, K. B., Callaghan, S., Jordan, T. H., Dieterich, J. H., and Field, E. H. Toward Physics-Based Nonergodic PSHA: A Prototype Fully Deterministic Seismic Hazard Model for Southern California. *Bulletin of the Seismological Society of America*, 111(2):898–915, Apr. 2021. doi: 10.1785/0120200216.

Milner, K. R., Shaw, B. E., and Field, E. H. Enumerating Plausible Multifault Ruptures in Complex Fault Systems with Physical Constraints. *Bulletin of the Seismological Society of America*, 112 (4):1806–1824, Aug. 2022. doi: 10.1785/0120210322.

Morris, P., Little, T., Van Dissen, R., Hemphill-Haley, M., Kearse, J., Hill, M., Vermeer, J., and Norton, K. A Revised Paleoseismological Record of Late Holocene Ruptures on the Kekerengu Fault Following the 2016 Kaikōura Earthquake. *New Zealand Journal of Geology and Geophysics*, 66(2):342–363, Apr. 2023a. doi: 10.1080/00288306.2022.2059766.

Morris, P., Little, T., Van Dissen, R., Hill, M., Hemphill-Haley, M., Kearse, J., and Norton, K. Evaluating 9 m of Near-Surface Transpressional Displacement during the M_w 7.8 2016 Kaikōura Earthquake: Re-Excavation of a Pre-Earthquake Paleoseismic Trench, Kekerengu Fault, New Zealand. *New Zealand Journal of Geology and Geophysics*, 66(2):244–262, Apr. 2023b. doi: 10.1080/00288306.2021.1954958.

Mouslopoulou, V., Saltogianni, V., Nicol, A., Oncken, O., Begg, J., Babeyko, A., Cesca, S., and Moreno, M. Breaking a Subduction-Termination from Top to Bottom: The Large 2016 Kaikōura Earthquake, New Zealand. *Earth and Planetary Science Letters*, 506:221–230, Jan. 2019. doi: 10.1016/J.EPSL.2018.10.020.

National Technology & Engineering Solutions of Sandia, LLC. Coreform Cubit. Coreform LLC, 2022.

Nicol, A., Van Dissen, R. J., Stirling, M. W., and Gerstenberger, M. C. Completeness of the Paleoseismic Active-Fault Record in New Zealand. *Seismological Research Letters*, 87(6):1299–1310, Nov. 2016. doi: 10.1785/0220160088.

Nicol, A., Khajavi, N., Pettinga, J. R., Fenton, C., Stahl, T., Bannister, S., Pedley, K., Hyland-Brook, N., Bushell, T., Hamling, I., Ristau, J., Noble, D., and McColl, S. T. Preliminary Geometry, Displacement, and Kinematics of Fault Ruptures in the Epicentral Region of the 2016 Mw 7.8 Kaikōura, New Zealand, Earthquake. *Bulletin of the Seismological Society of America*, 108(3B):1521–1539, 2018. doi: 10.1785/0120170329.

Nicol, A., Khajavi, N., Humphrey, J., Dissen, V., Gerstenberger, M., and Stirling, M. Geometries and Slip of Historical Surface- Rupturing Earthquakes in New Zealand and Their Application to Seismic Hazard Analysis. *EQC report*, 2022.

Nicol, A., Howell, A., Litchfield, N., Wilson, T., Bannister, S., and Massey, C. Introduction to the Kaikōura Earthquake Special Issue. *New Zealand Journal of Geology and Geophysics*, 66(2):137–146, Apr. 2023. doi: 10.1080/00288306.2023.2197240.

Nissen, E., Elliott, J. R., Sloan, R. A., Craig, T. J., Funning, G. J., Hutko, A., Parsons, B. E., and Wright, T. J. Limitations of Rupture Forecasting Exposed by Instantaneously Triggered Earthquake Doublet. *Nature Geoscience*, 9(February), 2016. doi: 10.1038/ngeo2653.

Nunn, P. D. Fished up or Thrown down: The Geography of Pacific Island Origin Myths. *Annals of the Association of American Geographers*, 93(2):350–364, June 2003. doi: 10.1111/1467-8306.9302006.

Ota, Y., Pillans, B., Berryman, K., Beu, A., Fujimori, T., Miyauchi, T., Berger, G., Beu, A., and Climo, F. Pleistocene Coastal Terraces of Kaikoura Peninsula and the Marlborough Coast, South Island, New Zealand. *New Zealand Journal of Geology and Geophysics*, 39(1):51–73, Mar. 1996. doi: 10.1080/00288306.1996.9514694.

Page, M. T. More Fault Connectivity Is Needed in Seismic Hazard Analysis. *Bulletin of the Seismological Society of America*, 111 (1):391–397, Feb. 2021. doi: 10.1785/0120200119.

Pizer, C., Clark, K., Howarth, J., Howell, A., Delano, J., Hayward, B. W., and Litchfield, N. A 5000 Yr Record of Coastal Uplift and Subsidence Reveals Multiple Source Faults for Past Earthquakes on the Central Hikurangi Margin, New Zealand. *GSA Bulletin*, Nov. 2023. doi: 10.1130/B36995.1.

Quigley, M., Mohammadi, H., Jiménez, A., and Duffy, B. Multi-Fault Earthquakes with Kinematic and Geometric Rupture Complexity: How Common? In *INQUA Focus Group Earthquake Geology and Seismic Hazards*, pages 316–318, New Zealand, 2017.

Quigley, M. C., Jiménez, A., Duffy, B., and King, T. R. Physical and Statistical Behavior of Multifault Earthquakes: Darfield Earthquake Case Study, New Zealand. *Journal of Geophysical Research: Solid Earth*, 124(5):4788–4810, May 2019.

doi: 10.1029/2019JB017508.

Reyners, M. Plate Coupling and the Hazard of Large Subduction Thrust Earthquakes at the Hikurangi Subduction Zone, New Zealand. *New Zealand Journal of Geology and Geophysics*, 41(4): 343–354, Dec. 1998. doi: 10.1080/00288306.1998.9514815.

Reyners, M., Eberhart-Phillips, D., and Bannister, S. Tracking Repeated Subduction of the Hikurangi Plateau beneath New Zealand. *Earth and Planetary Science Letters*, 311(1):165–171, Nov. 2011. doi: 10.1016/j.epsl.2011.09.011.

Richards-Dinger, K. and Dieterich, J. H. RSQSim Earthquake Simulator. *Seismological Research Letters*, 83(6):983–990, Nov. 2012. doi: 10.1785/0220120105.

Robinson, R. Potential Earthquake Triggering in a Complex Fault Network: The Northern South Island, New Zealand. *Geophysical Journal International*, 159(2):734–748, Nov. 2004. doi: 10.1111/j.1365-246x.2004.02446.x.

Robinson, R. and Benites, R. Synthetic Seismicity Models for the Wellington Region, New Zealand: Implications for the Temporal Distribution of Large Events. *Journal of Geophysical Research : Solid Earth*, 101(B12):27833–27844, 1996. doi: 10.1029/96JB02533.

Rollins, C., Gerstenberger, M. C., Rhoades, D. A., Rastin, S. J., Christophersen, A., Thingbaijam, K. K. S., Dissen, R. J. V., Graham, K., DiCaprio, C., and Fraser, J. The Magnitude–Frequency Distributions of Earthquakes in Aotearoa New Zealand and on Adjoining Subduction Zones, Using a New Integrated Earthquake Catalog. *Bulletin of the Seismological Society of America*, 114(1):150–181, Feb. 2024. doi: 10.1785/0120230177.

Rollins, C., Christophersen, A., Thingbaijam, K. K. S., Gerstenberger, M. C., Hutchinson, J., Eberhart-Phillips, D., Bannister, S., Van Dissen, R. J., Seebeck, H., and Ellis, S. An Integrated Earthquake Catalog for Aotearoa New Zealand (Version 1), Event-Type Classifications, and Regional Earthquake Depth Distributions. *Bulletin of the Seismological Society of America*, Apr. 2025. doi: 10.1785/0120230179.

Savage, J. C. A Dislocation Model of Strain Accumulation and Release at a Subduction Zone. *Journal of Geophysical Research*, 88 (B6):4984–4996, 1983. doi: 10.1029/JB088iB06p04984.

Schwartz, D. P. Review: Past and Future Fault Rupture Lengths in Seismic Source Characterization—The Long and Short of It. *Bulletin of the Seismological Society of America*, 108(5A):2493–2520, Oct. 2018. doi: 10.1785/0120160110.

Seebeck, H., Van Dissen, R. J., Litchfield, N. J., Barnes, P. M., Nicol, A., Langridge, R. M., Barrell, D. J. A., Villamor, P., Ellis, S. M., and Rattenbury, M. S. New Zealand Community Fault Model - Version 1.0. *GNS science report*, 2022. doi: 10.21420/GA7S-BS61.

Seebeck, H., Van Dissen, R., Litchfield, N., Barnes, P. M., Nicol, A., Langridge, R., Barrell, D. J. A., Villamor, P., Ellis, S., Rattenbury, M., Bannister, S., Gerstenberger, M., Ghisetti, F., Sutherland, R., Hirschberg, H., Fraser, J., Nodder, S. D., Stirling, M., Humphrey, J., Bland, K. J., Howell, A., Mountjoy, J., Moon, V., Stahl, T., Spinardi, F., Townsend, D., Clark, K., Hamling, I., Cox, S., De Lange, W., Wopereis, P., Johnston, M., Morgenstern, R., Coffey, G., Eccles, J. D., Little, T., Fry, B., Griffin, J., Townend, J., Mortimer, N., Alcaraz, S., Massiot, C., Rowland, J. V., Muirhead, J., Upton, P., and Lee, J. The New Zealand Community Fault Model – Version 1.0: An Improved Geological Foundation for Seismic Hazard Modelling. *New Zealand Journal of Geology and Geophysics*, pages 1–21, Mar. 2023. doi: 10.1080/00288306.2023.2181362.

Seequent. Leapfrog-Geo. A Bentley Systems Inc Company, 2024.

Shaw, B. E., Milner, K. R., Field, E. H., Richards-Dinger, K., Gilchrist, J. J., Dieterich, J. H., and Jordan, T. H. A Physics-Based Earthquake Simulator Replicates Seismic Hazard Statistics across California. *Science Advances*, 4(8):1–10, 2018. doi: 10.1126/sciadv.aau0688.

Shaw, B. E., Fry, B., Nicol, A., Howell, A., and Gerstenberger, M. An Earthquake Simulator for New Zealand. *Bulletin of the Seismological Society of America*, 112(2):763–778, Feb. 2022. doi: 10.1785/0120210087.

Stirling, M., McVerry, G., Gerstenberger, M., Litchfield, N., Van Dissen, R., Berryman, K., Barnes, P., Wallace, L., Villamor, P., Langridge, R., Lamarche, G., Nodder, S., Reyners, M., Bradley, B., Rhoades, D., Smith, W., Nicol, A., Pettinga, J., Clark, K., and Jacobs, K. National Seismic Hazard Model for New Zealand: 2010 Update. *Bulletin of the Seismological Society of America*, 102(4): 1514–1542, Aug. 2012. doi: 10.1785/0120110170.

Stirling, M., Goded, T., Berryman, K., and Litchfield, N. Selection of Earthquake Scaling Relationships for Seismic-Hazard Analysis. *Bulletin of the Seismological Society of America*, 103(6):2993–3011, Dec. 2013. doi: 10.1785/0120130052.

Stirling, M., Litchfield, N. J., Villamor, P., Dissen, R. J. V., Nicol, A., Pettinga, J., Barnes, P., Langridge, R. M., Little, T., Barrell, D. J., Mountjoy, J., Ries, W. F., Rowland, J., Fenton, C., Hamling, I., Asher, C., Barrier, A., Benson, A., Bischoff, A., Borella, J., Carne, R., Cochran, U. A., Cockroft, M., Cox, S. C., Duke, G., Fenton, F., Gasston, C., Grimshaw, C., Hale, D., Hall, B., Hao, K. X., Hatem, A., Hemphill-Haley, M., Heron, D. W., Howarth, J., Juniper, Z., Kane, T., Kearse, J., Khajavi, N., Lamarche, G., Lawson, S., Lukovic, B., Madugo, C., Manousakis, I., McColl, S., Noble, D., Pedley, K., Sauer, K., Stah, T., Strong, D. T., Townsend, D. B., Toy, V., Villeneuve, M., Wandres, A., Williams, J., Woelz, S., and Zinke, R. The Mw7.8 2016 Kaikōura Earthquake: Surface Fault Rupture and Seismic Hazard Context. *Bulletin of the New Zealand Society for Earthquake Engineering*, 50(2):73–84, June 2017. doi: 10.5459/bnzsee.50.2.73-84.

Stirling, M., Fitzgerald, M., Shaw, B., and Ross, C. New Magnitude–Area Scaling Relations for the New Zealand National Seismic Hazard Model 2022. *Bulletin of the Seismological Society of America*, Dec. 2023. doi: 10.1785/0120230114.

Tullis, T. E., Richards-Dinger, K., Barall, M., Dieterich, J. H., Field, E. H., Heien, E. M., Kellogg, L. H., Pollitz, F. F., Rundle, J. B., Sachs, M. K., Turcotte, D. L., Ward, S. N., and Burak Yikilmaz, M. A Comparison among Observations and Earthquake Simulator Results for the Allcal2 California Fault Model. *Seismological Research Letters*, 83(6):994–1006, Nov. 2012a. doi: 10.1785/0220120094.

Tullis, T. E., Richards-Dinger, K., Barall, M., Dieterich, J. H., Field, E. H., Heien, E. M., Kellogg, L. H., Pollitz, F. F., Rundle, J. B., Sachs, M. K., Turcotte, D. L., Ward, S. N., and Yikilmaz, M. B. Generic Earthquake Simulator. *Seismological Research Letters*, 83(6): 959–963, Nov. 2012b. doi: 10.1785/0220120093.

Ulrich, T., Gabriel, A. A., Ampuero, J. P., and Xu, W. Dynamic Viability of the 2016 Mw 7.8 Kaikōura Earthquake Cascade on Weak Crustal Faults. *Nature Communications 2019 10:1*, 10(1):1–16, Mar. 2019. doi: 10.1038/s41467-019-09125-w.

Upton, P., Tulloch, A. J., Crampton, J. S., Duvall, A. R., Eberhart-Phillips, D., Ellis, S. M., Sagar, M. W., Langridge, R. M., Townsend, D. B., and Harbert, S. A. Development of an Intracontinental Plate Boundary Transfer Zone, Marlborough, Aotearoa New Zealand: A Review and Synthesis. *Geological Society of America Bulletin*, 137(7-8):3368–3388, July 2025. doi: 10.1130/b37794.1.

Valentini, A. Allowing Multi-Fault Earthquakes and Relaxing Fault Segmentation in Central Apennines (Italy): Hints for Fault-Based PSHA. *Bulletin of Geophysics & Oceanography*, 62(4):647–668, 2021. doi: 10.4430/bgta0339.

Van Dissen, R. and Nicol, A. Mid-late Holocene Paleoseismicity of the Eastern Clarence Fault, Marlborough, New Zealand. *New Zealand Journal of Geology and Geophysics*, 52(3):195–208,

Sept. 2009. doi: 10.1080/00288300909509886.

Van Dissen, R. and Yeats, R. S. Hope Fault, Jordan Thrust, and Uplift of the Seaward Kaikoura Range, New Zealand. *Geology*, 19(4):393, 1991. doi: 10.1130/0091-7613(1991)019<0393:HFJTAU>2.3.CO;2.

Van Dissen, R., Seebeck, H., Wallace, L. M., Rollins, C., Gerstenberger, M. C., Howell, A., Di Caprio, C., and Williams, C. A. New Zealand National Seismic Hazard Model 2022: Geologic and Subduction Interface Deformation Models. *GNS science report*, 2022. doi: 10.21420/CEXY-AB93.

Van Dissen, R., Johnson, K. M., Seebeck, H., Wallace, L. M., Rollins, C., Maurer, J., Gerstenberger, M. C., Williams, C. A., Hamling, I. J., Howell, A., and DiCaprio, C. J. Upper Plate and Subduction Interface Deformation Models in the 2022 Revision of the Aotearoa New Zealand National Seismic Hazard Model. *Bulletin of the Seismological Society of America*, 114(1):37–56, Feb. 2024. doi: 10.1785/0120230118.

Walcott, R. I. Modes of Oblique Compression: Late Cenozoic Tectonics of the South Island of New Zealand. *Reviews of Geophysics*, 36(1):1–26, Feb. 1998. doi: 10.1029/97RG03084.

Wallace, L. M., Reyners, M., Cochran, U., Bannister, S., Barnes, P. M., Berryman, K., Downes, G., Eberhart-Phillips, D., Fagereng, A., Ellis, S., Nicol, A., McCaffrey, R., Beavan, R. J., Henrys, S., Sutherland, R., Barker, D. H. N., Litchfield, N., Townend, J., Robinson, R., Bell, R., Wilson, K., and Power, W. Characterizing the Seismogenic Zone of a Major Plate Boundary Subduction Thrust: Hikurangi Margin, New Zealand. *Geochemistry, Geophysics, Geosystems*, 10(10), 2009. doi: 10.1029/2009GC002610.

Wallace, L. M., Barnes, P., Beavan, J., Dissen, R. V., Litchfield, N., Mountjoy, J., Langridge, R., Lamarche, G., and Pondard, N. The Kinematics of a Transition from Subduction to Strike-Slip: An Example from the Central New Zealand Plate Boundary. *Journal of Geophysical Research: Solid Earth*, 117(B2):2405, Feb. 2012. doi: 10.1029/2011JB008640.

Wallace, L. M., Hamling, I. J., Kaneko, Y., Fry, B., Clark, K., Bannister, S. C., Ellis, S. M., Francois-Holden, C., Hreinsdottir, S., and Mueller, C. What Role Did the Hikurangi Subduction Zone Play in the M7.8 Kaikoura Earthquake? *AGU presentation*, 2017:S14B–04, Dec. 2017.

Wallace, L. M., Hreinsdóttir, S., Ellis, S., Hamling, I., D'Anastasio, E., and Denys, P. Triggered Slow Slip and Afterslip on the Southern Hikurangi Subduction Zone Following the Kaikōura Earthquake. *Geophysical Research Letters*, 45(10):4710–4718, 2018. doi: 10.1002/2018GL077385.

Walsh, E., Stahl, T., Howell, A., and Robinson, T. Two-Dimensional Empirical Rupture Simulation: Examples and Applications to Seismic Hazard for the Kaikōura Region, New Zealand. *Seismological Research Letters*, 94(2A):852–870, Mar. 2023. doi: 10.1785/0220220231.

Wang, T., Wei, S., Shi, X., Qiu, Q., Li, L., Peng, D., Weldon, R. J., and Barbot, S. The 2016 Kaikōura Earthquake: Simultaneous Rupture of the Subduction Interface and Overlying Faults. *Earth and Planetary Science Letters*, 482:44–51, Jan. 2018. doi: 10.1016/j.epsl.2017.10.056.

Wells, D. L. and Coppersmith, K. J. New Empirical Relationships among Magnitude, Rupture Length, Rupture Width, Rupture Area, and Surface Displacement. *Bulletin of the Seismological Society of America*, 84(4):974–1002, Aug. 1994. doi: 10.1785/BSSA0840040974.

Wessel, P., Luis, J. F., Uieda, L., Scharroo, R., Wobbe, F., Smith, W. H. F., and Tian, D. The Generic Mapping Tools Version 6. *Geochemistry, Geophysics, Geosystems*, 20(11):5556–5564, Nov. 2019. doi: 10.1029/2019gc008515.

Williams, C. A., Eberhart-Phillips, D., Bannister, S., Barker, D. H. N., Henrys, S., Reyners, M., and Sutherland, R. Revised Interface Geometry for the Hikurangi Subduction Zone, New Zealand. *Seismological Research Letters*, 84(6):1066–1073, Nov. 2013. doi: 10.1785/0220130035.

Wilson, J. M., Yoder, M. R., Rundle, J. B., Turcotte, D. L., and Schultz, K. W. Spatial Evaluation and Verification of Earthquake Simulators. In Zhang, Y., Goebel, T., Peng, Z., Williams, C. A., Yoder, M., and Rundle, J. B., editors, *Earthquakes and Multi-hazards Around the Pacific Rim, Vol. I*, pages 85–99. Springer International Publishing, Cham, 2018. doi: 10.1007/978-3-319-71565-0_7.

Wood, R. A., Pettinga, J. R., Bannister, S., Lamarche, G., and McMORRAN, T. J. Structure of the Hanmer Strike-Slip Basin, Hope Fault, New Zealand. *Geological Society of America Bulletin*, 106(11):1459–1473, Nov. 1994. doi: 10.1130/0016-7606(1994)106<1459:sothss>2.3.co;2.

Xu, W., Feng, G., Meng, L., Zhang, A., Ampuero, J. P., Bürgmann, R., and Fang, L. Transpressional Rupture Cascade of the 2016 M_w 7.8 Kaikoura Earthquake, New Zealand. *Journal of Geophysical Research: Solid Earth*, 123(3):2396–2409, Mar. 2018. doi: 10.1002/2017JB015168.

Zhang, L., Meng, G., and She, Y. The Spatiotemporal Properties of Afterslip Following the 2016 Kaikoura Earthquake in New Zealand from GPS Observations: Its Complementary and Inherited Patterns with Coseismic Slip. *Geophysical Journal International*, 242(2):ggae293, June 2025. doi: 10.1093/gji/ggae293.

Zinke, R., Hollingsworth, J., Dolan, J. F., and Van Dissen, R. Three-Dimensional Surface Deformation in the 2016 M_w 7.8 Kaikōura, New Zealand, Earthquake From Optical Image Correlation: Implications for Strain Localization and Long-Term Evolution of the Pacific-Australian Plate Boundary. *Geochemistry, Geophysics, Geosystems*, 20(3):1609–1628, Mar. 2019. doi: 10.1029/2018GC007951.